STUDY OF EBULLATED BED FLUID DYNAMICS FOR H-COAL. ANNUAL PROGRESS REPORT NO. 1, AUGUST 1, 1977-AUGUST 31, 1978

AMOCO OIL CO., NAPERVILLE, IL. RESEARCH AND DEVELOPMENT DEPT

FEB 1979

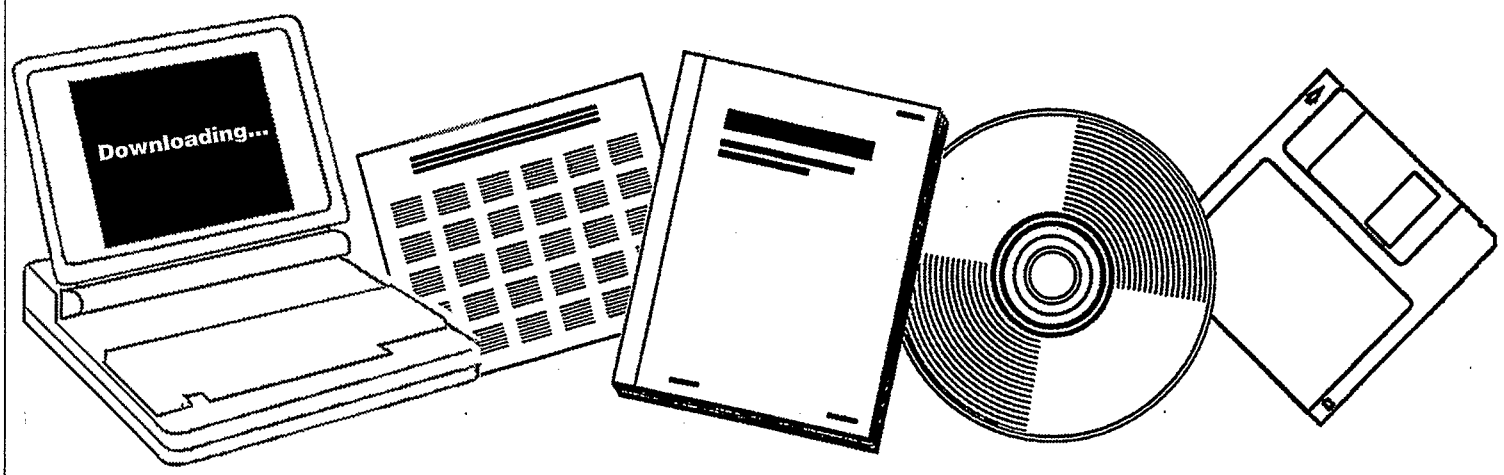

One Source. One Search. One Solution.

NTIS

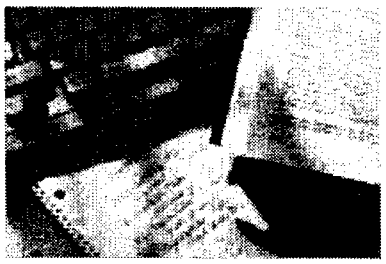

Providing Permanent, Easy Access to U.S. Government Information

National Technical Information Service is the nation's largest repository and disseminator of government-initiated scientific, technical, engineering, and related business information. The NTIS collection includes almost 3,000,000 information products in a variety of formats: electronic download, online access, CD-ROM, magnetic tape, diskette, multimedia, microfiche and paper.

Search the NTIS Database from 1990 forward

NTIS has upgraded its bibliographic database system and has made all entries since 1990 searchable on **www.ntis.gov.** You now have access to information on more than 600,000 government research information products from this web site.

Link to Full Text Documents at Government Web Sites

Because many Government agencies have their most recent reports available on their own web site, we have added links directly to these reports. When available, you will see a link on the right side of the bibliographic screen.

Download Publications (1997 - Present)

NTIS can now provides the full text of reports as downloadable PDF files. This means that when an agency stops maintaining a report on the web, NTIS will offer a downloadable version. There is a nominal fee for each download for most publications.

For more information visit our website:

www.ntis.gov

U.S. DEPARTMENT OF COMMERCE
Technology Administration
National Technical Information Service
Springfield, VA 22161

STUDY OF EBULLATED BED FLUID DYNAMICS FOR H-COAL

ANNUAL PROGRESS REPORT NO. 1
AUGUST 1, 1977-AUGUST 31, 1978

I. A. VASALOS, E. M. BILD, T. D. EVANS, J. W. JONES,
A. W. LARSON, S. E. SHIELDS, D. F. TATTERSON, A. P. VANDER KLAY

PREPARED FOR THE UNITED STATES
DEPARTMENT OF ENERGY
UNDER CONTRACT EF-77-C-01-2588

DATE PUBLISHED: FEBRUARY, 1979

FE-2588-18
M79-26

STUDY OF EBULLATED BED FLUID DYNAMICS FOR H-COAL

ANNUAL PROGRESS REPORT NO. 1
AUGUST, 1977-SEPTEMBER, 1978

I. A. VASALOS, E. M. BILD, T. D. EVANS, J. W. JONES,
A. W. LARSON, S. E. SHIELDS, D. F. TATTERSON, A. P. VANDER KLAY

DATE PUBLISHED: FEBRUARY, 1979

CONTRACT EF-77-C-01-2588

TABLE OF CONTENTS

TABLE OF CONTENTS

I -2-

TABLE OF CONTENTS

I -3-

TABLE OF CONTENTS

I -4-

FOREWORD

The H-Coal process, developed by Hydrocarbon Research, Incorporated (HRI), involves the direct catalytic hydroliquefaction of coal to low-sulfur boiler fuel or synthetic crude oil. The 200-600 ton-per-day H-Coal pilot plant is being constructed next to the Ashland Oil, Incorporated refinery at Catlettsburg, Kentucky under ERDA contract to Ashland Synthetic Fuels, Incorporated. The H-Coal ebullated bed reactor contains at least four discrete components: gas, liquid, catalyst, and unconverted coal and ash. Because of the complexity created by these four components, it is desirable to understand the fluid dynamics of the system. The objective of this program is to establish the dependence of the ebullated bed fluid dynamics on process parameters. This will permit improved control of the ebullated bed reactor.

The work to be performed is divided into three parts: review of prior work, cold flow model construction and operation, and mathematical modeling. The review of prior work has been completed. The objective of this first annual report is to review in detail the progress made in all three parts of the project during the first year.

OBJECTIVE AND SCOPE OF WORK

The overall objective of this project is to improve control of the H-Coal reactor through a better understanding of the hydrodynamics of ebullated beds. The project is divided into three main tasks:

1) Review of prior work in three-phase fluidization.
2) Construction of a cold flow unit and collection of data.
3) Development of a mathematical model to describe the behavior of gas/liquid fluidized beds. The model will be based on information available in the literature and on data generated in the cold flow unit.

Progress made on all three tasks during the first year of the project is presented in this report. A list of all publications previously issued in the past year is given in Table I.

SUMMARY OF PROGRESS TO DATE

Review of Prior Work

A key feature of the H-Coal process is the use of an ebullated bed for achieving good mixing between slurried coal, hydrogen, and extruded catalyst particles. The H-Coal reactor can be modeled as a four-phase fluid bed system containing liquid, fines, gases, and catalyst particles. For this reason, a review of the literature was undertaken to determine what data, models, and correlations exist for describing the behavior of liquid/solid, gas/solid, and gas/liquid/solid systems. The search also included a review of experimental techniques available to monitor multiphase fluidization and to measure physical properties of coal/oil mixtures. The results of the literature review were used to guide the experimental program and for the selection of experimental techniques to be used with the H-Coal fluid dynamics unit. The final report of the literature review issued on May 24, 1978.

Unit Construction

A cold flow model was constructed, with unit shakedown starting in May, 1978. The unit process design is very much along the lines of previous work conducted by Hydrocarbon Research, Incorporated (HRI). The unit consists of a glass reactor 6" in ID and 20' long. The reactor is made of four glass sections connected with metal spool pieces. A recycle cup located in the upper part of the reactor is used to separate the gas and liquid before the liquid is recycled to the bottom of the reactor. The fresh feed consisting of either pure liquid or coal slurry is mixed with the recycle stream and gas before entering the reactor. Downstream of the reactor, the liquid is separated from the gas and is returned to the feed tank. The gas can either be recycled to the reactor or be vented to the atmosphere. Unit instrumentation, pumps, compressors were selected largely based on in-house expertise. A key feature of the unit is a gamma-ray elevator on which a gamma-ray

Cs-137 source and a scintillation counter detector can simultaneously travel along the reactor. Pressure and sample taps inserted through the spool pieces provide additional information. The entire unit is monitored with a ModComp II mini computer. Visual displays (CRT) and a teletype increase the feedback of operating changes and have greatly increased the flexibility and expediency of data gathering.

Data Collection

The objective of this phase of work is to use liquids which at room temperature have physical properties (viscosity, density, surface tension) similar to those of H-Coal liquids at H-Coal reactor conditions. The following liquids have been selected: water, kerosene, toluene, and mineral oil. Nitrogen, helium, and Freon-12 are the gases selected. Coal char with particle size and density similar to the coal particles used in the H-Coal process is being used.

Characterization of the fluids and solids which will be used in the experimental program has started. The particle size distribution of the coal char and the catalyst particles was also obtained. Attempts were made to measure the viscosities of coal char slurries with a Brookfield SynchroLectric viscometer and a capillary tube viscometer.

Recognizing that measuring the properties of H-Coal liquids is very important for the ultimate use of the results from this study, a liquid sampling system was designed and built to obtain samples from HRI's PDU. The samples will be supplied to Battelle Research Institute for viscosity measurements.

In the cold flow unit, experiments with water, water/coal char slurries and kerosene have been completed. In all cases the American Cyanamid HDS-2A 1/16" x 3/16" catalyst extrudates were used. The gamma-ray scan data and weight of catalyst in the reactor are used for finding the bed height and catalyst volume holdup. The gamma-ray scan data are also used for finding the liquid holdup. The Richardson-Zaki correlation was used to evaluate gas/liquid data. The drift flux approach was used to evaluate gas/slurry/catalyst data. The effects of fluid viscosity were noted and some effects of coal fines on increasing liquid viscosity were identified.

REVIEW OF PRIOR WORK

A review of the literature for the H-Coal hydrodynamics project was completed in May, 1978. Three areas of literature were reviewed: 1) the hydrodynamics of fluidization; 2) experimental techniques for multiphase systems; and 3) the physical properties of coal/oil mixtures. The first area was reviewed to determine existing data, correlations, and models in two- and three-phase fluidized systems. This background provides a basis for planning experiments and developing a model of three-phase fluidized beds. The second area was reviewed to aid in the selection of experimental techniques to be used in the cold flow unit. The third area provides the background necessary to analyze the viscosity

of the liquid samples obtained from HRI's PDU.

Over 200 references in these three areas were reviewed. These are listed in Appendix D. Some of the highlights of the review will be presented below.

Hydrodynamics of Fluidization

This section contained a review of the literature in three areas: 1) liquid/solid fluidization; 2) gas/liquid vertical flow; and 3) gas/liquid/solid fluidization. The first two areas were reviewed because they represent the limiting cases of the three-phase system as the gas and solid volume fractions approach zero, respectively.

Liquid/Solid Fluidization.--This area has received much attention during the past thirty years. A large volume of data for different-sized spherical particles and liquids has been reported, and many methods of correlating the data have been proposed. Excellent reviews of these methods have been published by Garside and Al-Dibouni (5) and by Barnea and Mizrahi (1).

The most widely used correlation for liquid/solid fluidization data is that of Richardson and Zaki (6). They correlated the liquid volume fraction (ϵ_l) with the superficial liquid velocity (U_l) to the terminal settling velocity of a single particle (U_t). The relation is:

$$\epsilon_l^{\,n} = \frac{U_l}{U_t} \qquad (1)$$

Richardzon and Zaki found that:

$$n = f(Re_t, d/D) \qquad (2)$$

where: Re_t = particle Reynolds number based on U_t.
d/D = particle diameter/bed diameter

For non-spherical particles, n was also found to be a function of the particle shape. For turbulent Reynolds numbers (> 500):

$$n = 2.7K^{0.16} \qquad (3)$$

Where K is Heywood's (181) shape factor:

$$K = \pi/6\ d_s^3/d_p^3 \qquad (4)$$

where: d_s = diameter of a sphere with the same volume as the particle.
d_p = diameter of a circle of the same area as the projected particle when lying in its most stable position.

Another method of correlating liquid/solid fluidization data has been proposed by Barnea and Mizrahi (1). It is based on a relationship between a modified drag coefficient (C_{d_m}) and a modified particle Reynolds number (R_{e_m}). Barnea and Mizrahi argue that for multi-particle

systems the effective density and viscosity of the liquid phase changes due to the effects of the fluidized particles. They relate these changes to the solid volume fraction (ϵ_s) in the bed. Using these relations in a force balance on the particle system develops the following relationship between the drag coefficient and Reynolds number:

$$Cd_m = 0.63 + \frac{4.8}{\sqrt{Re_m}} \tag{5}$$

where: $$Re_m = Re\left(\frac{U_r/U_t}{Exp(5\epsilon_s/3[1 - \epsilon_s])}\right) \tag{6}$$

$$Cd_m = Cd\left(\frac{U_r}{U_t}\right)^2\left(\frac{1 - \epsilon_s}{1 + \epsilon_s^{1/3}}\right) \tag{7}$$

$$\frac{U_r}{U_t} = \frac{1}{1 + \epsilon_s^{1/3}}$$

Re = Reynolds number for a single particle.

Cd = Drag coefficient for a single particle.

HRI's (202,203) liquid/solid fluidization data were also reviewed and analyzed in terms of the Richardson-Zaki correlation.

The literature on non-Newtonian liquid/solid fluidization was reviewed. Only one paper (2) was found which involved fluidizing the bed with a slurry.

Vertical Gas/Liquid Flow.--The literature indicates that for the range of superficial gas and liquid flow rates of interest to three-phase fluidized systems, there are two gas/liquid flow patterns: 1) the ideal-bubbly regime, in which the bubbles rise as a uniform, steady cloud with little interaction; and 2) the churn-turbulent regime, which is a transition region between ideal-bubbly flow and fully developed slug flow. The churn-turbulent regime is dominated by bubble coalescence; hence, the bubble size is larger than in the ideal-bubbly regime, bubble wake effects became important, and the flow is unsteady. The transition between the ideal-bubbly flow regime and the churn-turbulent regime is very important in two- or three-phase chemically reacting systems. The interfacial area available for mass transfer is much greater in the ideal-bubbly regime.

The following categories were reviewed in vertical gas/liquid flow: bubble formation; rise velocity of single bubbles, bubble wakes, bubble coalescence, bubble breakup, swarms of bubbles, and slug behavior. Of particular importance are the categories of bubble coalescence and bubble breakup.

The relative rates of these two processes determine which gas/liquid flow regime (ideal-bubbly or churn-turbulent) dominates the flow pattern.

Bubble coalescence in gas/liquid flow is an extremely complex phenomenon. It can be dominated by surface phenomena or by the liquid flow pattern of the system. Particularly important to the latter are bubble wake effects and the liquid circulation pattern.

Numerous authors (42, 12, 185, 195) have studied the effects of surfactants on bubble coalescence. Bubble wake effects have been studied by Crabtree and Bridgewater (22).

Numerous authors (48, 36, 12, 17) have found that in bubble swarms of equal size, free from contaminant effects, the mechanism of coalescence becomes one of bubble clustering and the subsequent thinning of the film separating the bubbles. The global liquid circulation in the flow equipment is very important in the bubble clustering process. Large bubbles rising in the center of the flow equipment drag liquid along with them; this can result in a net downflow of liquid near the walls. This action imparts to the bubble at the bottom a radial velocity toward the center which aids the clustering process. Calderbank (17) found that the rate of coalescence increases greatly as the liquid viscosity increases. He argues that increasing the viscosity dampens the turbulence in the liquid, which allows the bubbles to conform more easily to the liquid flow pattern. This aids the bubble clustering process.

Far less work has been devoted to the study of bubble breakup. Clift and Grace (19) proposed that bubbles break up via a Taylor instability (59). Taylor has shown that for inviscid fluids, small disturbances on a horizontal surface between the fluids grow if the upper fluid is more dense than the lower fluid. In the case of bubbles, breakup can occur if the disturbance becomes sufficiently large.

Bellman and Pennington have extended Taylor's analysis to include the effects of liquid viscosity and surface tension on the rate of breakup.

Considerable work has been done in vertical bubble flow to determine the effect of neighboring bubbles on the rise velocity of a bubble. For the ideal-bubbly regime, several models have been proposed. These models relate the slip velocity of the bubble swarm (U_s) to the terminal velocity (U_t) of a single bubble and the gas holdup (ϵ_g). The slip velocity in a gas/liquid system is given by:

$$U_s = \frac{U_g}{\epsilon_g} - \frac{U_l}{1 - \epsilon_g} \tag{8}$$

where U_g and U_l are the superficial gas and liquid velocities, respectively. These models are usually defined in terms of the gas drift flux (V_{CD}), which is defined as:

$$V_{CD} = \epsilon_g(1 - \epsilon_g)\, U_s \tag{9}$$

The various models are:

1) Turner (60): $V_{CD} = U_t \epsilon_g(1 - \epsilon_g)$ (10)

2) Davidson and Harrison (24): $V_{CD} = U_t \epsilon_g$ (11)

3) Bridge (16): $V_{CD} = U_t \epsilon_g (1 - \epsilon_g)^n$ (12)

4) Marrucci (99): $V_{CD} = U_t \epsilon_g (1 - \epsilon_g)^2 / 1 - \epsilon_g^{5/3}$ (13)

For the churn-turbulent regime, only Zuber and Findlay (65) have proposed the following model:

$$V_{CD} = U_t \epsilon_g \quad (14)$$

Gas/Liquid/Solid Fluidization.--The addition of gas to a liquid fluidized bed increases the complexity of the system considerably. Many of these complexities have direct analogs in the corresponding two-phase systems. For instance, several authors (78,70) report the existence of two gas/liquid flow regimes in three-phase beds: the ideal-bubbly and churn-turbulent regimes. These have been referred to (78) as the "bubble-coalescing" regimes. Other complexities are unique to three-phase systems. Turner (105) was the first to report the contraction of some liquid fluidized beds upon the addition of gas. Steward and Davidson (103) and Ostergaard (93) have proposed mechanisms by which this contraction occurs.

The literature in this area was divided into the following sections: 1) bubble behavior in three-phase beds; and 2) data and correlation of three-phase systems.

The section on bubble behavior in three-phase beds covered the following areas: 1) rise velocity of single bubbles in three-phase beds; 2) bubble wakes; and 3) bubble coalescence and breakup in three-phase beds. The bed was found to have several unique effects in these areas. Several authors (71,85,108) found that the rise velocity of single bubbles was reduced by the presence of a bed. In order to explain this effect, they contend that the bed behaves as a high-viscosity fluid, with the viscosity of the bed declining as the bed expands. Massimilla (85) and Ostergaard (95) also observed that for a given bed particle size, the rate of bubble coalescence decreased with increasing bed expansion. This effect was also attributed to the bed behaving as a high-viscosity fluid; high viscosity favors coalescence.

Numerous authors (64,82,85,95,109) have also found a unique effect of bed particle size on the gas/liquid flow regime present in the bed. In general, small particles promote coalescence and reduce gas holdup. Hence, small particles favor the churn-turbulent (bubble coalescence) flow regime. Large particles, on the other hand, tend to reduce bubble coalescence and increase gas holdup. The majority of data on which the conclusions are based are for the air/water system. The data indicate that the critical particle size between coalescing and non-coalescing beds is between 3 and 4 mm.

Many investigators (98,86,68,69,109,78,80,66,87,67,90) have collected data on three-phase beds. A variety of gas/liquid/solid combinations were used in these investigations. A summary of these experiments is presented in Table II. Many of these investigators developed empirical correlations for volume fraction of the phases. These are summarized in Table III. In general, these correlations relate the volume fractions

to gas and liquid properties and the superficial flow velocities. It is recommended that these correlations be used only for the specific system for which they were developed.

Three models have been proposed to correlate three-phase fluidization data. These models attempt to take into consideration details of the bed structure such as bubble rise velocity or bubble wake volume. Often the relations describing these details are empirical.

Ostergaard (93) has proposed a model based on the assumption that the bed consists of a liquid fluidized phase (ϵ_l), a bubble phase (ϵ_g), and a wake phase (ϵ_w). The liquid fluidized phase consists of the solids and the liquid not contained in the wake phase. This is often referred to as the particulate phase. Ostergaard further assumed that the wake phase moves at the gas velocity and has the same porosity as the liquid fluidized phase.

Ostergaard presents empirical equations relating the bubble velocity (U_l), ϵ_g, ϵ_w, and ϵ_l to the superficial gas and liquid velocities. These equations have to be solved by an iterative procedure.

Darton and Harrison (70) have proposed a model which is based on the work of Stewart (104) and Efremov and Vakrushev (72). They propose that the bubble wakes are particle-free and that the liquid flux in the bubble wakes is given by $\bar{k}U_g$, where $\bar{k}$ is the mean value of the liquid/wake volume/bubble volume ratio. Darton and Harrison develop an empirical correlation for $\bar{k}$ as a function of U_l and U_g. The superficial liquid velocity and the liquid holdup in the particulate phase are given by $(U_l - \bar{k}U_g)/(1 - \epsilon_g - \bar{k}\epsilon_g)$ and $(\epsilon_l - \bar{k}\epsilon_g)/(1 - \epsilon_g - \bar{k}\epsilon_g)$, respectively. These expressions are used in conjunction with the Richardson-Zaki correlation to obtain a relation between ϵ_l and k, U_g, U_l, n, and ϵ_g.

In order to obtain a third relation, Darton and Harrison apply the drift flux approach discussed above in the section on gas/liquid flow to the three-phase system. They analyzed the data of Ostergaard and Michelson (86) in terms of the drift flux. A plot of V_{CD} vs. ϵ_g revealed two flow regimes: the ideal-bubbly and the churn-turbulent. Using this plot and the above two relations, the volume fractions of the various phases can be calculated from an iterative procedure.

Bhatia and Epstein (65) have also proposed a generalized wake model. Following Ostergaard (39), they also propose four distinct phases in the bed: solid, liquid, gas, and the wake phase. The solids concentration in the wake phase can be varied between zero and that in the particulate liquid/solid fluidized phase by means of an adjustable parameter, X_k. The value of X_k ranges between 0 and 1. The wake volume in the three-phase system is related to that in a gas/liquid two-phase system by an empirical function of solid holdup. The particulate liquid/solid phase is described by a Richardzon-Zaki type model. The model also takes into consideration the possible existence of two gas/liquid flow regimes in the bed. Bhatia and Epstein develop six equations for the six unknown

systems. Among the unknowns are the volume fractions of the various phases. These equations must also be solved using an iterative procedure.

Experimental Techniques for Multiphase Systems

Experimental techniques for measuring the properties of an ebullating bed involve devices which are either external or internal to the reactor. Internal devices will interfere to some degree with the fluid flow. Therefore, techniques which are external to the reactor are most desirable.

The literature on both types of techniques was reviewed. External techniques reviewed include gamma-ray scans, radioactive tracers (gas, liquid, and solid), and sonic probes. Internal techniques reviewed include light, impedance, and conductivity probes.

External Techniques

Gamma-Ray Scans.--This is an excellent technique for determining the average density in multiphase systems without causing flow disturbance. The use of gamma-rays is based on the differential absorption of radiation by various materials.

It has been shown by several investigators (66,147) that gamma-ray scans can be coupled with other measurements of multiphase systems to determine the volume fraction of each component in addition to the average density.

The two most popular gamma-ray sources used for scanning are Cs-137 and Co-60. Both sources have relatively high energy gamma-rays and long half-lives. Scintillation detectors with sodium iodide crystals have several advantages over other detection systems. They have higher detection efficiency, shorter resolving time, and can discriminate between gamma-rays of different energies.

Sonic Methods.--There are three basic sonic techniques: the Doppler shift, phase time, and dual path methods.

The dual path probe may be the most reliable when it can be used. The method is independent of changes in the speed of sound and thus also of temperature changes.

The Doppler shift method is used when there are particles or bubbles in the flow to scatter sound waves. The presence of these scatters would attenuate the signal for the other two methods.

Application of the phase time and dual path methods is dependent on the sonic impedance. It is proportional to the fluid density and the sound velocity in the fluid. In multi-phase systems, the two methods can be used only if the sonic impedances of the various phases are similar.

Tracers.--Gas, liquid, or solid tracers injected into a flow system can be used to determine the residence time distribution and flow profile for each phase.

There are several tracer-detector systems which can be used. Sampling techniques have several problems. Samples taken from the reactor may not be representative and sampling line effects may distort the results. The use of radioactive tracers which can be detected from outside the reactor circumvents these problems. To be detected from outside the reactor, the tracers must be gamma-ray emitters.

Michelson and Ostergaard (86) have used gas and liquid radioactive tracers to determine holdups in a three-phase fluidized bed. Two detectors were used to monitor the tracers. Two problems arose with the use of the argon gas tracer. It was absorbed in the liquid phase, and individual gas bubbles had different rise velocities. The tracer detected not only depends on the amount of tracer in the bubble, but also on the ratio of the amount of tracer to the rise velocity of the bubble. Because of these problems, only qualitative information on gas holdup was obtained.

Techniques Internal to the Reactor

Light Probes.--Several probes have been developed based on either light refraction or transmission through the fluid medium.

Refractive probes are based on the difference of the refractive index of the different fluids with which they are in contact. One probe developed by Jones and Delhaye (155, 145) is small and mobile, and thus will cause minimum flow disruption.

A typical application of the light transmission technique is the addition of dye to a fluid system. The progress of the dye is monitored with the light probe.

Impedance and Conductivity Probes.--Impedance probes are used for gas/liquid systems. When gas envelopes the probe, resistance increases. Probes with several contacts have been developed. Bubble size, velocity, and shape can be discerned if multicontact probes are used.

Conductivity probes are used when one of the phases is conductive or a conductive tracer has been added to the system. The progress of the conductive phase is then monitored.

Based on the review of techniques, gamma-ray scans were selected for use with pressure drop and bed height measurements to determine the holdup of each phase in the cold flow unit. Gas radioactive tracers will be used as well to determine gas holdup. A sonic technique was selected to monitor the coal fine concentration in slurries.

Physical Properties of Coal/Oil Mixtures

The literature in this area dealt exclusively with the measurement of viscosity. No literature on surface tension could be found.

The various papers reviewed indicated that the viscosity of coal/oil mixtures varies with base oil, temperature, volume per cent solids, and the size distribution of the suspended solids. Only two techniques were found which are capable of measuring the viscosity of coal/oil mixtures

at H-Coal reactor conditions. One technique involved pulling a bob through a concentric cylinder with a known force and measuring its velocity. The other technique involved a couette flow system consisting of a rotating cylinder in a stationary cup. These techniques were developed by Battelle Labs (177) and Exxon (209), respectively.

Empirical correlations for the viscosity of slurries were also reviewed.

CONSTRUCTION OF COLD FLOW UNIT AND DATA COLLECTION

A schematic diagram of the H-Coal fluid dynamics unit is shown in Figure 2. Design and construction for this unit were coordinated by the systems design group of Amoco Oil. Systems design incorporates elements of process design, mechanical design, instrumentation, automation, and computerization. Progress in the different areas is shown in Figure 1. Details on the work done in each area are given below.

Process Design

The process flow of the H-Coal fluid dynamics unit resembles that of the process development unit (PDU) built by HRI. The reactor consists of a 6" ID vessel 20' in length. The slurry is prepared in a 60-gallon tank. Other major vessels include: one 100-gallon feed tank, and a 60-gallon gas/liquid separator with a mist eliminator.

Three pumps are needed for the operation of the unit: 1) a transfer mixing pump for facilitating the slurry preparation and the transfer of the slurry to the feed pump; 2) a slurry feed pump for supplying the slurry to the reactor; and 3) a slurry recycle pump for internal slurry circulation in the reactor vessel. Under typical testing operating conditions, the slurry feed rate will amount to 3 GPM, while the slurry recycle pump will supply 15 GPM. The gas and liquid overflow from a 1" ID pipe located at the same level as the top of the recycle cup. The gas is separated from the liquid in the separator, D-3. Entrained liquid droplets accumulate in a demister located on top of the separator. The gas passes through Cooler E-2, and it can either be vented to the atmosphere through Valve PV-1 or can be directed to a gas recycle compressor. This flexibility is necessary because of the need to use gases such as Freon-12 and helium. The gas temperature is regulated with a heat exchanger, and it then combines with the total liquid stream before it returns to the reactor.

Mechanical Design

Support Structure.--The reactor and separator are supported on a steel structure with four levels. The reactor is supported in a 5' x 3' section in the center of the structure. The first level is three feet above ground level, and all other levels are nine feet apart. The structure covers a ground area of about 15.5' x 18.5'.

Reactor Components.--The reactor is constructed from four glass sections 5' in length and 6" in diameter. The glass sections are connected through flanges to five metal spool pieces. A schematic diagram of the assembled reactor is shown in Figure 3. The reactor is supported only from the bottom spool piece, which is bolted to a wide flange column. The bottom spool piece is also supported from underneath by a pipe column. The other spool pieces are used to guide the reactor along the support column. The piping connections at the top of the reactor are flexible. During the early phases of the program the reactor was secured to the column at each spool piece. This configuration put the glass sections under stress and resulted in breaking the bottom and top glass sections. After consultations with representatives of Owens-Illinois, the reactor was supported from the bottom spool piece while the glass was put under compression. The latter was accomplished with rods threaded to the spool pieces along the reactor length.

The spool pieces have entries for sample taps, pressure taps, and thermowells to monitor the system. A drawing of a spool piece is shown in Figure 4. As shown in Figure 4, the system is designed to insert two pressure taps through each spool piece. Thus, a total of eight ΔP measurements is feasible with this design. The lines are maintained clear by bleeding a low gas rate through each tap. It was found that gas flow caused vibrations in the impulse lines, which in turn created fluctuations in the ΔP measurements. As a result, new pressure taps were solidly inserted on each spool piece, making feasible the use of only four ΔP measurements. More details are given in the instrumentation section.

A sample probe can also be inserted into the reactor through each spool piece. A drawing of the sample probe assembly is shown in Figure 5. The probe is inserted into the reactor through a full-bore ball valve. A slot in the probe is aligned with another valve and sample container for sample removal. Samples of the slurry will be used to monitor the coal fines in slurry concentration along the reactor.

The reactor inlet distributor is shown in Figure 6. The distributor was modeled after the one used by HRI in the PDU. During the early phases of the program, problems were encountered with catalyst backflowing through the bubble cup and plugging the feed lines. Reducing the distance between the bubble cup and reactor bottom from 1/4" to 1/8" eliminated the plugging problems.

The recycle cup design is shown in Figure 7. The cup design is also similar to the one used by HRI. The recycle cup is connected to the downcomer with a section of flexible pipe. The recycle cup is spaced inside the glass with Teflon tabs to keep the cup from scratching the reactor. The cup is supported from the top spool piece with four thin steel pipes.

The glass reactor is enclosed in Lexan shielding to contain the glass reactor and contents if it fractures. The shield was constructed from

sheets of Lexan molded in half-cylinders. The sections are screwed together at the spool pieces and along the sides of the reactor. Sections of the shield can be removed to give access to the reactor.

Tanks.--The slurry preparation tank, D-2, is shown in Figure 8. The tank capacity of 60 gallons was sized so that slurry for the entire system could be made in two batches. The coal fines are added to the tank through a hooded feed hopper at the top of the tank. The hopper design is shown in Figure 9.

Feed Tank D-1 is shown in Figure 10. The 100-gallon tank holds the liquid inventory required to operate the fluid dynamics system. Both Tanks D-1 and D-2 have bafflers spaced at 90° inside the tank. The impeller systems were designed to maintain the coal fines in suspension.

Levels in the tanks are monitored using DP cells across the gas purge diplegs in the tanks. The diplegs also serve to keep the tanks blanketed with inert gas.

The separator design is shown in Figure 11. The separator was sized for about a 1.5-minute liquid residence time at maximum liquid flow rate. The separator level is also monitored using a DP cell across a gas purge dipleg. A mist eliminator is used on the gas exit from the separator to remove any entrained liquid. The eliminator is made in two sections with different-sized meshes to prevent plugging with coal fines if slurry droplets are entrained in the gas. The mesh is in a section of glass pipe to allow for visual observation. The glass demister section is shown in Appendix Figure A-1.

Gamma-Ray Elevator.--The elevator is designed so that a gamma-ray source and detector can travel vertically along the reactor to monitor the fluid dynamics of the system. The source and detector are supported on a Unistrut frame. The frame runs in Unistrut guides with Unistrut trolley wheels. The framework is adjustable so two detector/source combinations can be mounted up to three feet apart.

The total weight of the framework, source, detector, and shielding is about 300 lb. This is counterbalanced by two pieces of 4" round barstock which travel in tubing sleeves. The counterweights and framework are supported by a 1/4" pitch chain which is guided over a 48-tooth sprocket. A 1/2 HP motor connected to a 60" gear reducer runs the elevator system. Maximum speed of the elevator system is 30 ft/min. There are two safety stop buttons on each level of the steel structure for emergency stop of the elevator.

Compressor and Pumps.--A Corken reciprocating compressor, Model D-290K9, with a 5 HP motor was chosen for recycling gas. This compressor has a water-cooled aftercooler and a continuous pressure unloader. It is designed to pump 3.6 SCFM at 15 psig inlet and 60 psig outlet pressures. The compressor discharges into a capacity tank to damp out flow rate fluctuations.

March magnetic drive pumps, Model No. TE-7S-MD, were chosen for the feed, slurry recycle, and transfer pumps. These centrifugal pumps are magnetically coupled to the motor so there are no problems with liquids or gas leaking through a dynamic seal. Because of the magnetic coupling design of this pump, it will not uncouple from the motor, so motor stoppage is not a problem. At a head of 20 psi, the pump will deliver about 20 GPM.

Other mechanical design drawings are shown in Appendix A.

Systems Design

Process variables are measured and controlled with state-of-the-art instruments of select industrial type. In general, the instrumentation was chosen on the basis of proven performance on similar operating pilot plants. In addition, critical items were bench-checked as received to spot any manufacturing flaws before plant startup.

Modular instrument cabinets located in an enclosed, air-conditioned corridor adjacent to the pilot plant house all process controllers, recorders, digital indicators, annunciators, critical switches, and circuit breakers. The corridor provides a clean environment that improves instrument performance, minimizes their maintenance, and encourages the operator to spend more time at the consoles evaluating plant performance.

Components.--A Honeywell TDC-2000 microprocessor-based system is used for controlling slurry feed and slurry recycle flows, gas flow, gas/liquid separator level, and reactor pressure. Dual-pen analog recording is provided for hard copy of these process variables. Analog displays of variables, set points, and valve positions are also provided.

A keyboard data entry panel allows the operator and electronic technicians to display and change set points, high and low limits, proportional bands, and reset rates. Although Honeywell electronic control loops have been used on other Amoco Oil pilot plants, this is the first plant where a digital control system has been incorporated.

In the remainder of this section, techniques for monitoring flow, pressure, temperature, tank levels, and other peripheral instrumentation systems will be discussed.

Flow Measurement.--A Nusonics Model 8000 meter was chosen to monitor slurry feed flow rate. The difference in frequency of sonic beams propagated axially to the flow is correlated with flow rate. A MicroMotion flow meter is used to measure slurry recycle flow rate. The deflection of this U-shaped flow tube due to the Coriolis-type acceleration of the flowing liquid is correlated with the mass flow rate. This flow meter was selected because tests show that entrained gases which are well

dispersed do not affect flow measurement and entrained gases are expected in the recycle line. A Nusonics Model 6180 concentration analyzer was chosen for continuous monitoring of the coal concentration in the slurry feed. The gas flow is monitored with a Honeywell Model 41105 differential pressure transmitter with an integral orifice assembly. The DP across the orifice is dependent on the gas velocity.

As shown on the system design drawing attached to this report, the discharges from the feed and recycle pumps flow through separate control valves and flow transmitters before joining ahead of the reactor distributor. A Young heat exchanger is used to maintain temperature control of the combined stream before entering the reactor.

The Dover Model 1020 split-body control valves with pneumatic positioners and interchangeable stellite valve trims are performing well in slurry service. These valves are globe-type and incorporate a streamlined flow passage to reduce erosion-inducing turbulence inside the body.

Valve bypasses are provided, but the control valves are not isolated for removal during operation.

March magnetic-drive centrifugal pumps (Model TE-7SMD) were chosen for the slurry flows. They are used with Chemloy bushings to reduce slurry erosion. Several other pumps were also considered--e.g., Crane Chempump, Moyno screw, and Tuthill rotary pumps. However, the March pumps were selected because the magnetic coupling eliminates seal problems and because the cost is considerably lower. Pump details were given in the mechanical design section.

Valving flexibility was provided to return the discharge flow from each pump back to the 60-gallon slurry mixing tank. An electronic Toledo Model 2184 scale with digital resolution to 0.1 gram is used for preparation of the coal slurries and calibration checks of the flow transmitters.

Recycle gas flow from the Corken D-290 compressor or once-through gas flow from cylinders is maintained constant using a Research Control valve with pneumatic positioner. The compressor operates via continuous pressure unloading with a variable differential pilot valve. The valve opens when the discharge pressure reaches a preset value and admits gas to the diaphragm unloader assemblies on the inlet check valves and holds them open. The compressor then runs unloaded at full speed until the discharge pressure reaches a low preset value. The pilot valve closes, releasing the pressure from the unloaders, and the inlet valve resets. A 30-gallon-capacity tank was installed at the discharge of the compressor to dampen compressor fluctuations and smooth recycle flow.

Level Measurement--Separator.--Separator level control utilizes a Honeywell Model 41105 diffused silicon differential pressure transmitter with electronic damping. A small flow of process gas (N_2, He, or Freon-12) is bubbled through the dipleg in the separator to keep the impulse line to the high-pressure side of the transmitter clean. The level control valve is also a Dover split-body type.

Pressure.--A three-element control loop with a Honeywell Model 412 pressure transmitter and Research Controls valve maintains a constant pressure on the glass reactor. To accommodate both the gas recycle and once-through cases, two control valves and two gas meters are installed. When the recycle compressor is being used, only a small amount of gas--up to a maximum of 10 SCFH--is released from the pilot plant. A Singer-American Meter wet test meter is used to measure this gas. For the once-through case, the released gas is measured via a Singer-American Meter dry test meter with capacity up to 300 SCFH. After metering, the gas is vented via a 1 1/2" tubing run through the roof of the pilot plant bay area. Discharges from pressure relief valves and rupture disks are directed to a blowdown drum for liquid containment and the off-gas vented via another 1 1/2" tube through the roof.

Pressure drop measurements along reactor sections are made to determine the average ebullated bed three-phase volume fraction. Bournes Model 5020 differential pressure transmitters with high speed of response were chosen for this function. Analog recorders used are: a three-pen Gould/Brush Model 2600 with 100 mm scales for the critical high-speed measurements; and two three-pen Texas Instruments Servo/Riters with overlapping pens on a 10" grid. All three recorders feature multiple chart speeds for maximum flexibility.

A small, continuous bleed of feed gas through each 1/8" ID pressure tap impulse line is used to keep the lines free of catalyst or slurry. Should the lines become plugged, however, a high-pressure gas surge can be initiated manually via three-way solenoid valves in the purge lines.

Originally, eight DP measurements were made with the taps spaced about 27" apart. However, the first series of pilot plant tests indicated that recorder pen sweeps were too large to obtain meaningful data. The data fluctuations were due to the vibration of the DP impulse lines within the reactor. A liquid-filled impulse line without purge flow was tried, but was unsuccessful because of catalyst and slurry plugging.

Thermowell taps in each spool piece are now being utilized for the differential pressure measurements. This eliminated the impulse line vibration problem, but reduced the number of differential pressure measurements to four. The DP across each five-foot reactor section is now being monitored.

Temperature.--Process and coolant temperatures are displayed digitally via a 1° resolution Doric indicator and recorded on a Honeywell Model 112 24-point recorder.

Gamma-Ray Scan Systems.--The gamma-ray system attached to the elevator used for scanning the reactor was obtained from Harshaw and K-Ray. The scintillator detection system was manufactured by Harshaw. A NaI scintillation crystal closely coupled to the photomultiplier tube (PMT) and preamplifier is mounted on the elevator. Other components used are: a stabilized amplifier/single-channel analyzer, high-voltage source for the PMT, and a rate meter. The scan output is monitored using a Texas

Instruments recorder on the panel board. Ten millicuries of Cs-137 from K-Ray is used as the gamma-ray source. Using the elevator system, the reactor can be scanned continuously from the bottom spool piece to the recycle cup.

An Ortec scintillation detection system and a Cs-137 source are used to scan the liquid recycle line from the recycle cup at the bottom of the reactor. The components used in this system are the same as in the Harshaw system except that the amplifier/single-channel analyzer does not have the stabilizer option. A vertical length of pipe is scanned. The system is used to monitor the quantity of entrained gas in the recycle liquid. The output is recorded with a Leeds and Northrup recorder.

Automation and Safeguard Systems

The H-Coal pilot plant was designed to operate semi-automatically. Non-routine operations such as startup, shutdown, catalyst changing, sampling, and feed preparation are handled manually. However, certain key operating sequences and "safeguarding" functions are automated using a Texas Instruments 5TI programmable logic control system.

Printout of digital gas meter readings for checking flow consistency is controlled via timer circuitry, but can be done "on demand". An automated package successfully used for driving movable thermocouples axially inside a reactor was adapted to moving the gamma-ray scan elevator. Three modes of operation allow total flexibility. The operator can dial a selected position on his control panel, push a button, and the elevator will move to that location. Also, he can option the scanner to move up and down continuously between limit switches. Finally, the scanner can move in pre-selected increments stepwise along the length of the reactor. This last mode is normally controlled by the ModComp II mini computer, but may be controlled via the localized automation.

Safeguarding of process equipment and personnel and plant status information is automated and identified. Process flows, pressures, levels, temperatures, and plant status are monitored continuously with sensors and limit switches for deviations from specified values. Any violations are identified individually on a Monitronix annunciator on the control cabinet. Additionally, certain violations result in the programmable controller activating circuit breakers, solenoid valves, or other control elements to effect shutdowns. Although the pilot plant was designed initially for day-shift operation only, minor changes have been incorporated so that the plant can run unattended overnight. Because of the large inventory of flammable liquid, we have installed a heat sensor to detect a fire and a liquid level sensor in the spill tank under the reactor. Should these be activated, light water extinguishers will blanket the floor and the spill tank. Additionally, a fire alarm will sound in the utility center, which is attended at all times, and at the local fire department. Any other alarms occurring during unattended operation will alert personnel in the utility center and be acknowledged as time permits.

Computerization

Computer Hardware Configuration.--The general hardware configuration for the computerization of the AU-77H pilot plant is shown in Figure 12. All equipment in the top half of the figure is located in the High Bay computer room. The peripherals portrayed in the lower half are located at the pilot plant control panel three hundred feet away from the computer room. All of these remote peripherals are connected to the computer via dedicated telephone lines. The lines have been found very reliable with transfer rates up to 9600 baud without error or conditioned lines. On the serial analog-to-digital converter (ADC), however, a set of line drivers have been installed strictly to isolate the computer and the ADC from each other. The computer control system (CCS), the multi-counter register (MCR), and the binary switches are multiplexed on a parallel data bus to the computer. This saves wiring costs by having only one parallel bus. The major equipment itself is described below.

ModComp II Computer: The computer is a general-purpose 16-bit processor with 128K bytes of memory. It employs a dual moving head disc with 5196K bytes of storage capacity. The software operating system is configured as a real-time multi-task system with a partition for off-line batch jobs. This batch task, however, may be checkpointed to disc if any real-time programs need the core to run. Also, all output to unit typers is fully buffered by first spooling the output to disc. In this manner, if the computer becomes inoperable for any reason, no output would be lost. This computer is equipped with asynchronous ports for serial devices such as CRT's and teletypes and with digital I/O for interfacing with the parallel data bus.

Tektronix 4662 Plotter: This device is used to generate user plots off-line for numerous applications. It is driven by the Tektronix Plot 10 software package, which contains the following features: automatic coordinate transformations (linear, logarithmic, and polar); virtual plotting; relative plotting; segmented line drawing; character generation allowing unlimited control of character size and slant; scaling and rotating of relative virtual vectors. Besides being used for graphic representation of test results, the plotter is also used for generating graphic displays similar to those produced by the Intelligence Systems Corporation (ISC) color graphic CRT, thus allowing "hard copy" of CRT displays. An example of this feature is shown in Appendix B.

ISC 8001G Color Graphic CRT: This peripheral is employed for real-time display of unit data. The CRT has eight colors, which may be used as foreground or background colors, with which graphic displays are generated of the pilot plant. When these displays are output to the CRT, real-time data--which are scanned every minute--are inserted at appropriate locations on the screen. An additional useful feature is a software refresh of data in real-time. In this way the data are kept current and trends are easy to spot. Also, this refresh feature can be

used effectively when lining out the unit. The following displays are currently implemented:

1) Pilot plant flow chart with major equipment labelled.
2) List of all current computer-scanned data points with their latest value and their conversion factors.
3) Pilot plant temperature displayed on unit flow chart.
4) Pilot plant pressures displayed on unit flow chart.
5) Pilot plant flows and levels displayed on unit flow chart.
6) Instructions on using the CRT and what displays are implemented.

Amoco Analog-to-Digital Converter: This in-house-designed ADC converts process signal analog inputs to digital values which are transmitted serially to the computer. Presently only 32 of the possible 256 signals are being used. Several of these signals are used as standards to correct the ADC for drift caused by ambient atmospheric changes.

Binary Switches and Watchdog Timer: The binary switches are used to relay event information to the computer of an on/off nature. Some of the manual switches are for Start of Test, End of Test, and Start Gamma-Ray Scan. Some of the on-line switches are Gamma-Ray Traverser Moving, At Home, and At Top. The watchdog timer will sound an alarm signifying the computer is down if it not reset within a certain length of time by the computer.

Amoco Computer Control System: The Amoco CCS is an in-house-designed system to interface with digital outputs both for relays and for TTL* circuits. The CCS controls the gamma-ray traveling scintillator counter (traverser). In order to accomplish this, the computer tells the CCS that it wants the traverser to go up or down to a certain hardware position. The CCS in turn interfaces to a 5TI programmable controller which synthesizes the proper signal to the traverser motor.

Amoco Multi-Counter Register: The Amoco MCR is employed for counting pulses and sending a binary coded decimal result to the computer on request. One channel of the MCR is used to monitor the position of the elevator for the gamma-ray scan. Each turn of the elevator motor sends a number of pulses to the MCR corresponding to how far the traverser has moved. Also, the MCR is used to count pulses from the scintillator counters (the one on the traverser and the one on the slurry recycle). Because of the feature which allows the operator to change the delta time for counting scintillator pulses, two MCR registers are used to count up to 99999999 before data overflow.

The interaction of these preceding devices to perform a gamma-ray scan is shown in Appendix B.

Computer Software Configuration.--The ModComp II computer used for monitoring the AU-77H pilot plant is running under MAX II/III, which is a vendor-supplied executive system. This system was generated to provide real-time multi-task execution and still provide a partition where off-line jobs and development work can be done. By giving real-time tasks

---

*0-5 volt signal.

priority based on their importance, time critical applications are easily implemented. One feature included in this operating system is checkpointing. This allows real-time tasks to usurp core from the background or off-line partitions and then return background to where it left off when execution is finished.

In addition to this ModComp-supplied operating system, several tasks have been added to the system environment which implement some very useful features. First of all, there is an output spooler which buffers all hard-copy output to the fast-access discs first before outputting to the slow hard-copy devices. This performs two functions: it allows real-time tasks to write to a hard-copy device without waiting and tying up core while the device is printing; and if the system should be abnormally halted for some reason in the middle of typing out a report, when the system is restarted the output will continue from where it left off without losing any output.

Another feature added to the system is the process operator communications program (POC). This program provides the following options to the unit operator through the unit's teletype:

1) Display the latest scanned value of a point automatically every five minutes or one time only.
2) Display or change the calibration factors used to convert analog signals to engineering units.
3) Display or change the high, low, or jump limit for a particular point.
4) Inhibit computer scan of a particular point and, if desired, assign a manual reading until normal scan is restored.
5) Set software "switches".

The output spooler and the POC program were written by Standard Oil R&D and are used on all pilot plant computers on site.

Also added to the system was a graphic color CRT package. This package includes a monitor program to direct CRT activity, a display program which puts current data in a display before transmission to the CRT, and an interactive graphing program which allows eight color graphic displays to be generated interactively by a user with simple commands. Some of the graphic displays currently implemented are described in the hardware configuration section. Besides generating real-time graphic displays, the CRT is used to activate several tasks at the operator's request such as the zero gamma-ray scan and the test initialization program.

All of the "system" programs provide a base for application programs specific to the AU-77H pilot plant. A generalized flow chart of the applications software configuration is shown in Figure 13. All of the programs are written primarily in Fortran with subroutine calls to assembly language subroutines. An exception to this is Program TSC, which operates the traveling scintillation counter. This program is written with a mixture of Fortran and assembly language. A brief description of each major applications program follows.

Program ZER: This program is activated by the operator by the CRT to complete a desired number of gamma-ray scans and average the results. This is done when the reactor contains only liquid to obtain a base for comparison when running tests with catalysts. These averaged scans are stored in a location on disc corresponding to that liquid being studied (water, mineral oil, kerosene, or toluene), and are then picked up by end-of-test calculation programs.

Program BEG: Program BEG is activated through the CRT by the operator when he is ready to start a new test. The operator is then interrogated as to test variables and then sets a software flag to allow a start of test.

Program A77: This is the scan-and-convert program for the pilot plant. It is activated automatically every minute. Upon activation, A77 checks for start-of-test indicator; scans and converts process inputs; checks high, low, and jump limits for each scanned point; keeps five-minute average of points; and initializes, begins, and monitors the traveling gamma-ray scan. A list of all scanned points is given in Table V.

Program TSC: This program drives the traveling scintillator counter or gamma-ray scan. Before activation, the calling program must initialize the following variables: step size, equilibrium time to wait after stopping before starting count, and the delta time during which the scintillator count is taken. During a test, these variables are set by the operator through the POC program, which is in turn picked up by A77, which initializes the variables and activates TSC to start the scan.

Program R77: Program R77 merely keeps a running test average of all scan points. It also checks for the end-of-test switch and activates the end-of-test Program F77.

Program F77: This is the end-of-test program. It takes the averaged test data and completes calculations using test variables initialized by Program BEG. Gamma-ray scan data are processed using test data and zero-scan data for the medium being studied. Then an end-of-test report is printed on the unit's typer and the test results are saved for later use. An example of an end-of-test report is shown in Appendix B.

Off-Line Programs: After a test there are several plots that can be obtained using the test data. Additionally, several general-purpose programs have been developed to generate plots as shown in the hardware and software configuration figures. Examples of plots from test data are shown in Appendix B.

DATA COLLECTION

Physical Properties of Liquids and Solids

The objective of the experimental program is to establish the hydrodynamic properties of the H-Coal reactor. Typical operating conditions of the H-Coal reactor and properties of the liquids at actual operating conditions are shown in Table VI. In the present work, liquids will be used

which at about room temperature have properties similar to those of the slurries shown in Table VI. The properties of the selected liquids are shown in Tables VII and VIII. The surface tension of the liquids was measured as a function of temperature. These results are reported in Table VIII. A Fischer Scientific surface tensiometer (Model 20) was used. The results indicate that surface tension varies linearly with temperature over the temperature range studied.

In addition to the viscosities of the pure liquids reported in Table VII, an effort was made to measure the viscosities of liquid coal char slurries. Two different methods were tried. The viscosities of toluene or mineral oil slurries containing 7 and 14 vol% coal char fines were measured with a Brookfield SynchroLectric viscometer with a UL adapter. The measured viscosities declined with time, indicating that the coal char particles are settling out in the viscometer.

A capillary tube viscometer having an ID of 1.6 mm and a length of 100 cm was then constructed to measure the viscosity of the coal char slurries. The viscometer was placed on a small auxiliary unit which had been constructed. A schematic diagram of the experimental setup is shown in Figure 14. When used to measure the viscosities of slurries, the capillary tube tended to plug. The tube was reamed out and appeared to perform satisfactorily. Measuring slurry viscosities started at the end of August, 1978.

The particle size distribution of the catalyst and coal char is also important in determining the hydrodynamic properties of the H-Coal reactor. The cumulative size distribution of the coal char particles which will be used to make slurries under this study was measured by IIT Research Institute using an optical microscope interfaced with a Quantimet 720 computerized image analyzer. The distribution is reported in Table IX. The geometric mean particle diameter is 3.4 microns.

The catalyst particle size distribution has also been measured. The lengths of catalyst chosen for this study are 1/8", 3/16", 1/4", and 3/8"; the diameter of the catalyst is 1/16". The catalyst has been supplied by American Cyanamid. Cyanamid has guaranteed that the variation of length does not exceed ± 20% for each of the above lengths. The length distribution for the 1/8", 3/16", 1/4", and 3/8" long catalyst is listed in Table X.

Unit Data

Experimental test conditions for the runs completed during the first year are reported in Table XI. All experiments listed in Table XI were run at a temperature of about 70°F. A summary is shown below:

Run	Liquid	Catalyst	Fines Concentration, Vol%
100	Water	HDS-2A, L=3/16",D=1/16"	0
101	Water	" "	1
102	Water	" "	5
200	Kerosene	---	0
201	Kerosene	HDS-2A, L=3/16",D=1/16"	0

Experimental data on catalyst bed heights and gamma-ray scans for water and water/slurry tests--Runs 100, 101, and 102--are reported in Tables XII, XIII, and XIV, respectively. Experimental data for kerosene--Runs 200 and 201--are given in Tables XV and XVI. Due to foaming in the recycle cup with kerosene, the recycle pump could not be used at high gas flow rates, thus limiting the total liquid flow with kerosene to 76.3 gpm/ft^2. Plots of bed expansion vs. liquid and gas flow rate are given in Figures 15, 16, 17, and 18 for Runs 100, 101, 102, and 201, respectively. In general, liquid flow rate has a much greater effect on increasing bed expansion than does gas flow rate. However, increasing coal fine concentration appears to enhance the effect of gas flow rate on bed expansion. For Run 102, with water/5 vol% coal fines, at high liquid flow rates, increasing gas velocity has a much greater effect on bed expansion than for any other run. This effect may result from the increased viscosity of the 5 vol% coal slurry.

Phase Holdups

Phase holdups calculated from bed height and gamma-ray measurements for Runs 100, 101, 102, 200, and 201 are given in Tables XVII through XXVI. The methods used to calculate ϵ_c, ϵ_l, and ϵ_g are given in Appendix C. Plots of the catalyst holdup, ϵ_c, as a function of liquid and gas flow rates are given in Figures 19, 20, and 21 for Runs 100, 101, and 102, respectively. As shown with the plots of bed expansion, liquid flow rate has a much greater effect on ϵ_c than gas flow rate. From these results, there is some indication that bed contraction is occurring. For several tests there was a significant increase in catalyst holdup with increasing gas flow rate. The catalyst holdup then decreased again with increasing gas flow. As discussed in the literature review, it has been proposed that this bed contraction occurs because of the formation of wakes behind the gas bubbles which move through the bed at the bubble velocity. This reduces the liquid velocity in the rest of the bed, thus causing it to contract. As the gas flow rate is further increased, the catalyst bed may again expand.

Correlations

The data on phase holdups were analyzed using two correlations--one for liquid/catalyst systems, and the other for gas/liquid/catalyst and the kerosene gas/liquid data.

Liquid/catalyst data were analyzed using the Richardson-Zaki correlation. Their analysis equates sedimentation with fluidization. The correlation relates the liquid volume fraction due to bed expansion to the ratio of the superficial liquid velocity to the terminal velocity of a single particle:

$$\epsilon_l^{\,n} = U_l/U_t \qquad (15)$$

$$n = f(Re_t, d/D) \qquad (16)$$

The functional form of n, the Richardson-Zaki index for ranges of Reynolds numbers, is given in Figure 22.

U_t was determined experimentally for water and kerosene at a temperature of 70°F. The soaked catalyst particles were dropped several feet in the liquid to determine U_t. For water, U_t was found to be equal to 0.42 ft/sec, and for kerosene, U_t equals 0.53 ft/sec.

U_t can also be determined from plots of $\ln \epsilon_l$ vs. $\ln U_l$ by extrapolating to $\epsilon_l = 1$. The plots for Runs 100-201 are shown in Figure 23. The terminal velocities determined from the plots do not agree with experimentally determined values. This discrepancy will be discussed below.

The Richardson-Zaki index, n, was determined by plotting the liquid holdup ϵ_l vs. U_l/U_t on log/log graph paper; 1/n is the slope of the line. The plots for Runs 100, 101, 102, and 201 are shown in Figures 24, 25, 26, and 27.

The results from tests with water and a 1 vol% coal fine/water slurry are very similar. The terminal velocities are about 0.4 ft/sec and the Richardson-Zaki indices are 2.1 and 2.3, respectively.

With the addition of 5 vol% coal to the water, the effect of increased viscosity should be observed. However, the terminal velocity for Run 102 increased to 0.45 ft/sec as determined from Figure 23, although it should decrease with increasing viscosity. The terminal velocity can also be calculated from the following equation for cylindrical geometry:

$$U_t = \sqrt{\frac{\pi d(\rho_c - \rho_l)g}{2\,\rho_l\,C_D}} \qquad (17)$$

C_D is inversely proportional to Re_t. Therefore, as viscosity increases, U_t should decrease. This result indicates that the error in determining U_t from the figure is greater than the effect of this increase in viscosity.

The Richardson-Zaki index increased from about 2 to 3 with the addition of 5 vol% coal fines. The index increased as expected due to the relationship given in Figure 22.

Kerosene is more viscous and less dense than water, and these changes in fluid properties would affect flow characteristics. The experimentally measured terminal velocity for kerosene-soaked catalyst particles is 0.53 ft/sec. The terminal velocity as determined from Figure 23 is 0.56 ft/sec. The terminal velocity of catalyst particles in water is about 0.42 ft/sec; thus, the catalyst terminal velocity increased in changing from water to kerosene. As seen in Equation 17, U_t will increase as the liquid density decreases. Apparently the change in density offset the change in viscosity which would have caused the terminal velocity to decrease compared with water.

The Richardson-Zaki coefficient for kerosene tests was 2.9--greater than the value of about 2.2 found for water. The change in viscosity and density both acted to decrease Re_t; thus, according to the relationship

in Figure 22, n increases. The Richardson-Zaki indices for all tests are given in Table XXVII.

The Richardson-Zaki index was calculated for both water and kerosene using the equations shown in Figure 22. Re_t was calculated for two different cases: dp as either the equivalent spherical diameter or as the cylinder diameter. The results are shown in Table XXVIII for a temperature of about 70°F. For both water and kerosene, the value used for dp had little effect on the calculated index. For water, the calculated values of n were just greater than the value found experimentally, and for kerosene, the calculated values were slightly low. However, the differences are within experimental error, indicating that these equations predict the index fairly well.

Gas/liquid and gas/liquid/catalyst flow data were analyzed using the drift flux method. For gas/liquid flow, drift flux (V_{CD}) is defined as:

$$V_{CD} = U_g(1 - \epsilon_g) - U_l\epsilon_g$$

Several models have been proposed to correlate drift flux with the terminal velocity of a single bubble and the gas holdup. These models were reviewed in a literature search which was issued as a separate report under this contract. The kerosene gas/liquid data analyzed with the drift flux method are plotted in Figure 28 with these other models. The Nicklin data shown in the figure are for air/water results. As expected, the data for kerosene fall on a line of lower slope than the water data. The drift flux at a given gas holdup decreases because the increased viscosity of kerosene causes the gas bubbles to rise at a lower velocity than in water.

The gas/liquid/catalyst flow data were analyzed using the Darton-Harrison drift flux approach. For three-phase systems, the drift flux is defined as:

$$V_{CD} = U_g(1 - \epsilon_g) - \frac{U_l\epsilon_g}{\epsilon_l}(1 - \epsilon_g)$$

Two flow regimes can be identified on plots of V_{CD} vs. ϵ_g: the ideal-bubbly (bubble disintegrating) and churn-turbulent (bubble coalescing). Data for Runs 100, 101, and 102 are shown in Figures 29, 30, and 31. Results from Runs 100 and 101 are very similar. The transition from ideal-bubbly to churn-turbulent flow occurred at higher gas velocities as the liquid velocity increased, except for the liquid velocity of 0.05 ft/sec. This liquid velocity is below minimum fluidization velocity, accounting for the anomaly.

Very little difference between Runs 100 and 101 would be expected because 1 vol% coal fines should have almost no effect on fluid properties. With the 5 vol% coal/water slurry (Run 102), in general the transition to the churn-turbulent flow occurred at gas flow rates greater than 0.05 ft/sec, whereas for Runs 100 and 101 the transition did not occur until gas flow rates greater than 0.10 ft/sec were achieved. The addition of coal fines increases the slurry viscosity. These results indicate that at higher

liquid viscosity, coalescence is enhanced. Calderbank, et al. (17) also noted a similar effect for gas/liquid flow. Transition from ideal-bubbly to the churn-turbulent regime depends on the relative rates of bubble coalescence and breakup. Increasing bubble coalescence will favor the transition from ideal-bubbly to churn-turbulent flow.

The Darton-Harrison drift flux approach illustrated in Figure 29 has been very useful in identifying flow transition. It is evident that for each experimental system, data will fall in either ideal bubbly region, churn turbulent, or in the transition region. From the limited work conducted to date, there is not yet an understanding of how the physical properties or operating conditions affect the flow regime. However, it is believed that successful use of Darton-Harrison approach will require a correlation relating $\bar{k}$ (ratio of wake to bubble volume) for the systems studied.

Measurement of Physical Properties of H-Coal Liquids

As part of the H-Coal fluid dynamics project, Amoco is attempting to measure the viscosity of liquid samples obtained from the PDU. These measurements are being made to determine if the viscosity of the liquids selected for study in Amoco's cold flow unit are in the same range as the viscosity of H-Coal liquids at H-Coal reactor temperatures and pressures.

Amoco plans to make these viscosity measurements on a subcontract basis. Various industrial laboratories and firms were contacted to determine their capabilities for measuring the viscosity of H-Coal slurries under reactor conditions (800-900°F, 2000-3000 psi). In Table XXIX, the laboratories contacted and the techniques they use to measure viscosity are listed.

Battelle Laboratories was selected to make the measurements, and Amoco signed a contract with them in August, 1978 to make the measurements. The cost of the measurements is $17,200. Battelle will measure the viscosity of four different slurry samples. These determinations are to be made at no less than four temperatures, ranging from 700 to 900°F and at pressures ranging from 2000 to 3000 psi of hydrogen.

Battelle has pointed out that they expect coking (polymerization) problems to develop with the H-Coal samples at high temperatures (300-400°C). This expectation is based on their previous experience in measuring the viscosity of Synthoil samples. In these measurements it was found that at high temperatures viscosity changed with time, thus indicating that the sample is physically changing in some manner.

A sampling system to obtain samples from HRI's PDU reactor was designed, constructed, and shipped to HRI. The system is shown in Figure 32. It is designed to operate at temperatures up to 900°F and pressures up to 3000 psi. It consists of a slop vessel, a sample vessel, an outage vessel, an HEX-SDV31A valve, and connecting lines.

A sample will be obtained in the following manner:

1) The sample and outage vessels will be evacuated and the valves between them closed.

2) The heaters will be brought up to temperature (400°F) and the slop vessel and connecting lines purged with nitrogen.

3) The HEX valves will be closed and the block valves to the PDU line will be opened; line pressure will be determined.

4) The HEX valve will be opened and the slop vessel filled.

5) The valves to the sample vessel will be opened and the sample vessel will be filled and sealed.

6) The block valves on the PDU line will be closed and the sample lines and slop vessel vented.

7) The system will be purged and drained with nitrogen.

8) After cooling to room temperature, the sample and outage vessels will be removed and the valves between them opened.

9) The sample and outage vessels will be shipped to Battelle for viscosity measurement.

HRI and Amoco have agreed that the sample point on the PDU will be between the external separator and the first-stage pressure letdown valve before the atmospheric flush.

Sampling of the PDU is scheduled to begin in September, 1978. In addition, to the four samples taken for Battelle, two additional samples will be taken for Oak Ridge National Laboratories.

COSTS

The total cost at the end of the first year was about $426,000. Most of this cost was used for constructing the unit. Total material cost charged to this program was about $132,000 as of the end of August, 1978. In Figure 33 the actual monthly charges are plotted versus month in project. The actual project costs are slightly lower than past projections for several reasons: 1) the work on viscosity measurements of H-Coal liquids by Battelle has not been carried out due to lack of samples from the PDU reactor; 2) very expensive equipment was given to the project by Amoco Oil for temporary use. In all, the project costs are well within expectations. No project overrun is anticipated.

FUTURE PLANS

1) Continue experiments with kerosene. Levels of coal fines and gas type will be varied.

2) Start experimental plan to determine significant effects.

3) Perform initial set of experiments with radioactive tracer gas Argon-41.

4) Continue measurements of coal slurry viscosity with the capillary tube viscometer.

5) Complete implementation of computer monitoring and evaluation of pilot plant operations.

CONCLUSIONS

Understanding the hydrodynamic behavior of the H-Coal reactor is the main objective of this project. To that end, a literature search was completed which reviewed all information related to the fluid dynamics behavior of gas/liquid/solid systems. A topical report on the subject was issued in May, 1978. Concurrently with the literature search, a cold flow model including a glass reactor 6" in diameter and 20' high was constructed. The process design of this unit followed practices established by HRI in their process development unit.

The cold flow model will be used to conduct experiments with gas and liquid slurries which at room temperature have similar properties to those of the H-Coal liquids at reactor conditions. The volume fraction occupied by gas/liquid slurries and catalyst particles will be determined by several experimental techniques. The use of a mini computer for data collection and calculation has greatly accelerated the analysis and reporting of data. Data on nitrogen/water/HDS catalyst and coal char fines were presented in this report.

Correlations identified in the literature search were utilized to analyze the data. From this analysis it became evident that the Richardson-Zaki correlation adequately describes the effect of liquid flow rate on catalyst expansion. The effect of coal char fines can be accounted for by the effect it has on the liquid viscosity. For the gas/slurry/catalyst and the water/nitrogen systems, a model developed by Darton and Harrison was used to analyze the data. Since the data base developed thus far is very limited, it is very difficult to evaluate the general applicability of this model. However, as more data are obtained, the model will be tested and will either be validated or replaced by another model.

Recognizing that the ultimate implementation of this work will require the development of a mathematical model, continuing emphasis will be placed on identifying the proper correlation describing the H-Coal reactor fluid dynamics. Because the use of this correlation will depend on knowledge of the viscosity of the H-Coal liquid at H-Coal reactor conditions, an effort was made to obtain samples from the HRI PDU reactor for viscosity determination by the Battelle Institute. Successful completion of this phase of the work will be emphasized.

Successful completion of this work will largely depend on the operability of the unit with slurries containing coal char concentrations up to 20 wt%. Although a carefully designed experimental plan has been set

up, operability performance will determine whether this statistically designed set of experiments will be followed up. Since the major goal of this program is to be of use to the H-Coal project, the experimental runs will emphasize this objective throughout the rest of the program life.

NOMENCLATURE

		Typical Units
A	Cross-sectional area of column	cm^2
C_D	Drag coefficient for single particle or bubble	--
C_{DM}	Drag coefficient for multi-particle system	--
d	Particle diameter	cm
$\bar{d}$	Average particle diameter	cm
d_e	Equivalent spherical diameter of bubble	cm
d_p	Diameter of a circle if the same area as the projected particle when lying in its most stable position	cm
d_s	Diameter of a sphere with the same volume as the particle	cm
d_{sm}	Sauter-mean bubble diameter	cm
D	Bed or tube diameter	cm
D_c	Diameter of capillary	cm
f	Frequency of formation of bubble cluster	sec^{-1}
Fr	Froude number	--
g	Acceleration of gravity	cm/sec^2
G	Dimensionless group	--
H_{GL}	Three-phase bed height	cm
H_L	Liquid/solid bed height	cm
j_l	Liquid flux	gm/cm^2 sec
j_l^*	Dimensionless liquid flux	--
$\bar{k}$	Average of wake volume to bubble volume ratio	--
K	Shape factor	--
K'	Effective hydrodynamic volume of particle	cm^3
l	Particle length	cm
M	Morton number	--
M'	Rheological parameter	$gm/cm\ sec^{n'-2}$

		Typical Units
n	Richardson-Zaki index or exponent in ideal bubbly flow regime models	--
n'	Rheological parameter	--
Q_g	Gas volumetric flow rate	cm^3/sec
r	Particle or bubble radius	cm
r^*	Dimensionless particle radius	--
r_e	Equivalent spherical bubble radius	cm
r_o	Orifice radius	cm
R	Radius of curvature	cm
Re	Particle Reynolds number	--
Re_b	Bubble Reynolds number	--
Re_f	Minimum fluidization particle Reynolds number	--
Re_m	Reynolds number for multi-particle system	--
Re_t	Particle Reynolds number based on U_t	--
U_b	Bubble rise velocity	cm/sec
U_g	Superficial gas velocity	cm/sec
U_l	Superficial liquid velocity	cm/sec
U_m	Mean velocity	cm/sec
U_r	Relative velocity between particles and liquid	cm/sec
U_s	Gas/liquid slip velocity	cm/sec
U_t	Terminal velocity of an isolated particle or bubble	cm/sec
U_{lo}	Superficial liquid velocity at incipient fluidization	cm/sec
U_{sl}	Velocity of gas slug	cm/sec
U_l'	Superficial liquid velocity in the particulate fluidized phase in a three-phase system	cm/sec
v_b	Bubble volume	cm^3

		Typical Units
v_{cD}	Gas drift flux	cm/sec
We	Weber number	--
X_k	Ratio of solids holdup in wake to solids holdup in particulate phase	--

Greek

β	Number of small bubbles forming a cluster	--
ϵ	Bed voidage	--
ϵ_g	Volume fraction of gas	--
ϵ_l	Volume fraction of liquid	--
ϵ_s	Volume fraction of solids	--
ϵ_w	Volume fraction of wake phase	--
δ	Pore diameter of gas distributor	cm
ρ_g	Gas density	gm/cm^3
ρ_s	Density of particles	gm/cm^3
ρ_l	Density of liquid	gm/cm^3
ρ_b	Density of fluidized bed	gm/cm^3
τ_w	Wall shear stress	$dynes/cm^2$
μ_e	Effective viscosity	poise
μ_l	Liquid viscosity	poise
σ	Surface tension	dynes/cm
λ	Wavelength of disturbance	cm
ϕ	Solids volume fraction	--

TABLE I

LIST OF PUBLICATIONS DURING THE FIRST YEAR

Vasalos, I. A., et al., Monthly Progress Report No. 1, FE-2588-1, October, 1977.

Vasalos, I. A., et al., Monthly Progress Report No. 2, FE-2588-2, November, 1977.

Vasalos, I. A., et al., Quarterly Progress Report No. 1, FE-2588-3, December, 1977.

Vasalos, I. A., et al., Monthly Progress Report No. 4, FE-2588-4, January, 1978.

Vasalos, I. A., et al., Monthly Progress Report No. 5, FE-2588-5, February, 1978.

Vasalos, I. A., et al., Quarterly Progress Report No. 2, FE-2588-7, March, 1978.

Vasalos, I. A., et al., Monthly Progress Report No. 3, FE-2588-8, April, 1978.

Vasalos, I. A., et al., Monthly Progress Report No. 8, FE-2588-9, May, 1978.

Vasalos, I. A., et al., H-Coal Fuild Dynamics Topical Report Part I: Literature Search, FE-2588-6, May, 1978.

Vasalos, I. A., et al., Quarterly Progress Report No. 3, FE-2588-10, June, 1978.

Vasalos, I. A., et al., Monthly Progress Report No. 10, July, 1978.

Vasalos, I. A., et al., Monthly Progress Report No. 11, August, 1978.

TABLE II

SUMMARY OF DATA FOR GAS/LIQUID/SOLID FLUIDIZATION

Investigators	System	Particle Size	Experimental Unit	Parameters Studied	Quantities Measured
1) Razumov, Manshilin, Nemets (98)	Air/Water/Sand Air/Water/Slag Beads	0.493 to 1.27 mm	300 mm Diameter Column	U_g, U_l	ϵ_s
2) Michelsen, Ostergaard (86)	Air/Water/Glass Beads	1,3,6 mm	5" Diameter Column	U_g, U_l, Particle Size	ϵ_s, ϵ_l
3) Dakshinamurty, Subramanyam, Rao (68,69)	Air/Water/Various Spherical Particles Air/Kerosene/Various Spherical Particles	1.06 to 6.8 mm	56 mm Diameter Column	Particle Size and Density σ, U_g, U_l	ϵ_s
4) Viswanathan, Kakai, Murti (109)	Air/Water/Quartz Particles Air/Water/Glass Beads	0.928,0.649 mm 4 mm	50.8 mm Diameter Column	U_g, U_l, Particle Size	ϵ_l, ϵ_g
5) Kim, Baker, Bergougnou (78)	Air/Water/Glass Beads Air/Water/Irregular Gravel	6 mm 2.6 mm	26 x 1" Rectangular Channel	U_g, U_l	ϵ_l, ϵ_g, Bubble Size and Velocity
6) Kim, Baker, Bergougnou (80)	Air-Water/Acetone-Glass Beads Air-Water/Acetone-Irregular Gravel Air-Sugar/Water-Glass Beads Air-Carboxymethyl Cellulose/Water-Glass Beads Air-Sugar/Water-Irregular Gravel Air-Carboxymethyl Cellulose/Water-Irregular Gravel	1,6 mm 2.6 mm 1,6 mm	26 x 1" Rectangular Channel	μ_l, σ, U_l, U_g	ϵ_g, ϵ_l
7) Blum and Toman (66)	Nitrogen/Light Mineral Oil	See Table II	4" Diameter Column	U_l, U_g, μ_l	ϵ_s
8) Nemets, Razumov, and Manshilin (87)	Air/Water/Sand Air/Heptane/Sand Air-Water/Glycerol-Sand	0.820 mm	90 mm Diameter Column	U_l, U_g, μ_l	ϵ_l, ϵ_g
9) Bruce, Revel-Chion (67)	Air/Water/Glass Spheres	2,4,6,8 mm	46.3 mm Diameter Column	U_l, U_g	ϵ_s, Bubble Size
10) Ostergaard, Theisen (90)	Air/Water/Glass Ballotini	0.28 to 2.2 mm	2 and 4" Diameter Column	U_l, U_g	ϵ_s

DFT/ml
2/20/78

TABLE III

EMPIRICAL CORRELATIONS FOR THREE-PHASE BEDS

Author	Correlation	Gas/Liquid	Solids (Dimension)	Column Diameter or Dimensions	Comments
Kim, Baker, Bergougnou (78)	$(\varepsilon_l)_{U_g=0} - \varepsilon_l = 0.0025 \left(Fr_l \frac{\rho_s}{\rho_l}\right)^{0.149} \left(Fr_g \frac{\rho_s}{\rho_s}\right)^{0.161} \left(\frac{Re_l}{Re_g}\right)^{0.259}$	Air/Water	Glass Beads (6 mm) Irregular Gravel (2.6 mm)	26" x 1"	Empirical, no consideration for bed contraction
	$(\varepsilon_l)_{U_g=0} = 0.409(Fr_l \rho_s/\rho_l)^{0.193}(Re_l)^{0.074}$				
Kim, Baker, Bergougnou (80)	$(\varepsilon_l+\varepsilon_g) = 1.40(Fr_l)^{0.17}(We)^{0.078}$ (Expanding Beds)				Empirical for expanding and contracting beds
	$(\varepsilon_l+\varepsilon_g)_{U_g=0} = 1.3(Fr_l)^{0.128}(We)^{0.073}\exp[0.31\, U_l/U_g(\varepsilon_l)_{U_g=0}]$ (contracting beds)	Air/Sugar Solutions Air/Carboxymethyl Cellulose Solution Air/Water Acetone	Glass Beads (6,1 mm) Irregular Gravel (2.6 mm)	26" x 1"	
	$(\varepsilon_l)_{U_g=0} = 1.353(Fr_l)^{0.208}(Re_l)^{-0.1}$				
	$\varepsilon_l = 1.54(Fr_l)^{0.234}(Fr_g)^{-0.088}(Re_l)^{-0.082}(We)^{0.082}$				
Dakshinamurty, Subrahmanyam, Rao (68,69)	$(\varepsilon_g + \varepsilon_l) = \left(K \frac{U_l}{U_t}\right)^m \left(\frac{\mu_l U_g}{\sigma}\right)^n$ $n = 0.08$ $K = 2.12,\ m = 0.41,\ Re_t < 500$ $K = 2.65,\ m = 0.6,\ Re_t > 500$	Air/Water Air/Kerosine	Numerous Diameters 1.06 to 6.8 mm	56 mm Diameter	Empirical, no consideration for bed contraction
Blum, Toman (66)	$\frac{(\varepsilon_g + \varepsilon_l) - (\varepsilon_l)_{U_g=0}}{1 - (\varepsilon_l)_{U_g=0}} = f(U_g)$	Nitrogen/Light Mineral Oil	Cylinders Dia. / Length 1/8" / 1/8" 3/16" / 3/32" 3/16" / 3/16"	4" Diameter	Empirical, no consideration for bed contractions
Razumov, Manshilin, Nemats (98)	$\varepsilon_s = 0.578 - 3.198\, U_l - 0.538\, U_g$ $\varepsilon_l = 0.422 + 0.135\, U_l/\bar{d}^{0.882} - 1.82\, U_g$ $\varepsilon_g = K(1 - \varepsilon_s)^{2.09}(U_g/U_l)^{0.78}$	Air/Water	Sand, Slag Beads 0.49 to 1.27 mm	300 mm	Empirical, no consideration for bed contractions

DFT/ml
2/20/78

TABLE IV

SCOPE OF AUTOMATIC SAFEGUARD ACTIONS--H-COAL PILOT PLANT AU-77H

M79-26/-36

Alarm Station Iden.	Trouble	Automatic Safeguard Action	Alarm/Action Delay	Alarm Switch	Override Switch	Scope Overri
PAH-1 HI PRESSURE KNOCK-OUT TRAP	Pressure In Knock-Out Trap D-6 Is Too High.	Alarm, stop slurry feed pump (pump 1), slurry recycle pump (pump 2), and gas recycle compressor (pump 3); bypass reactor via diverter valves FV-4 and FV-5. (Pumps must be restarted manually and valves must be repositioned manually.)	5 sec	PSH-1	PAS-1A	Alarm.
PAL-1 LO PRESSURE KNOCK-OUT TRAP	Pressure In Knock-Out Trap D-6 Is Too Low.	Alarm, stop slurry feed pump (pump 1), slurry recycle pump (pump 2), and gas recycle compressor (pump 3). (Pumps must by restarted manually.)	5 sec	PSL-1	PAS-1B	Alarm; safeguard actions.
PAL-2 LO PRESSURE BUILDING N2	Pressure In Nitrogen Feed Line Is Too Low.	Alarm.	--	PISL-2	PAS-2	--
PAL-3 LO PRESSURE HEL/FREON CYLINDERS	Pressure In Helium/Freon-12 Feed Gas Cylinders Is Too Low.	Alarm.	--	PISL-3	PAS-3	--
PAH/L-4 HI/LO PRESS REACTOR	Pressure At Top of Reactor Is Too High Or Too Low.	Alarm.	5 sec	PISH/L-4	PAS-4	Alarm.

TABLE IV (Continued)

Alarm Station Iden	Trouble	Automatic Safeguard Action	Alarm/Action Delay	Alarm Switch	Override Switch	Scope of Override
PAHH-5 HI-HI PRESS REACTOR	Pressure At Top Of Reactor Has Reached The Second High Limit.	Alarm, stop slurry feed pump (pump 1), slurry recycle pump (pump 2), and gas recycle compressor (pump 3); bypass reactor via diverter valves FV-4 and FV-5. (Pumps must be restarted manually and valves must be repositioned manually.)	5 sec	PISHH-5	PAS-5A	Alarm.
PALL-5 LO-LO PRESS REACTOR	Pressure At Top Of Reactor Has Reached The Second Low Limit.	Alarm, stop slurry feed pump (pump 1), slurry recycle pump (pump 2), and gas recycle compressor (pump 3). (Pumps must be restarted manually.)	5 sec	PISLL-5	PAS-5B	Alarm; safeguard actions.
PAH/L-6 HI/LO PRESS SLURRY RECYCLE	Pressure In Slurry Recycle Pump Discharge Line Is Too High Or Too Low.	Alarm.	5 sec	PSH/L-6	PAS-6	Alarm.
LAH/L-1 HI/LO LEVEL SEPARATOR	Level Of Slurry In Separator D-3 Is Too High Or Too Low.	Alarm.	15 sec	LSH/L-1	LAS-1	Alarm.
LAHH-2 HI-HI LEVEL SEPARATOR	Level Of Slurry In Separator D-3 Has Reached the Second High Limit.	Alarm, stop slurry feed pump (pump 1) and slurry recycle pump (pump 2). (Pumps must be restarted manually.)	10 sec	LISHH-2	LAS-2	Alarm.
LAH/L-3 HI/LO LEVEL FEED TANK D-1	Level Of Slurry Feed In Feed Tank D-1 Is Too High Or Too Low.	Alarm.	--	LISH/L-3	LAS-3	Alarm.
LAH/L-4 HI/LO LEVEL PREP TANK D-2	Level Of Slurry Feed In Prep/Calibration Tank D-2 Is Too High Or Too Low.	Alarm.	--	LISH/L-4	LAS-4	Alarm.

TABLE IV (continued)

Alarm Station Iden	Trouble	Automatic Safeguard Action	Alarm/Action Delay	Alarm Switch	Override Switch	Scope of Override
LAH-5 HI LEVEL KNOCK-OUT TRAP	Liquid Has Been Detected In Knockout Trap At Recycle Compressor Inlet.	Alarm	--	LISH-5	LAS-5	Alarm.
LAH-6 HI LEVEL SPILL TANK	Reactor Breakage Has Dumped Coal Slurry And Catalyst Into Spill Tank.	Alarm, blanket the tank with light water extinguisher foam via FV-7. (Valve must be closed manually.)	--	LISH-6	LAS-6	--
FAH/L-1 HI/LO FLOW SLURRY FEED	Flow Of Slurry Feed Is Too High (Check Operability Of Flow Valve) Or Too Low (Check For Line Plugging).	Alarm.	5 sec	FSH/L-1	FAS-1	Alarm.
FAH/L-2 HI/LO FLOW SLURRY RECYCLE	Flow Of Slurry Recycle Is Too High (Check Operability Of Flow Valve) Or Too Low (Check For Line Plugging).	Alarm.	5 sec	FSH/L-2	FAS-2	Alarm.
FAH/L-3 HI/LO FLOW RECYCLE GAS	Flow Of Recycle Gas Is Too High Or Too Low.	Alarm.	5 sec	FSH/L-3	FAS-3	Alarm.
FAL-4 LO FLOW OFF GAS	Flow Of Off Gas From Separator Is Too Low-- Check Pressure Tap Bleeds.	Alarm.	--	FSL-4 (5TI)	FAS-4	Alarm.
AAH/HH-1 OXYGEN AT RECYL COMP INLET	Oxygen Has Been Detected At The Inlet To Recycle Compressor (Pump 4).	Alarm. On second high limit, additionally stop slurry feed pump (pump 1), slurry recycle pump (pump 2) and gas recycle compressor (pump 3). (Pumps must be restarted manually.)	--	ASH/HH-1 (0.1/0.3)	AAS-1	Alarm.

TABLE IV(Continued)

Alarm Station Iden	Trouble	Automatic Safeguard Action	Alarm/Action Delay	Alarm Switch	Override Switch	Scope of Override
JA-1 SLURRY FEED PUMP STOPPED	March Slurry Feed Pump (Pump 2) Has Stopped.	Alarm.	--	JY-1	JAS-1	Alarm
JA-2 SLURRY RECYLE PUMP STOPPED	March Slurry Recycle Pump (Pump 3) Has Stopped.	Alarm.	--	JY-2	JAS-2	Alarm.
JA-3 RECYCLE GAS COMP STOPPED	Corken Recycle Gas Compressor (Pump 4) Has Stopped.	Alarm.	--	JY-3	JAS-3	Alarm.
JA-4 SLURRY FEED MIX STOPPED	Slurry Feed Tank D-1 Mixer Has Stopped.	Alarm.	--	JY-4	JAS-4	Alarm.
TAL-1 LO TEMP SLURRY-GAS FEED	Temperature of Combined Slurry Feed And Recycle and Gas Recycle Is Too Low--Check E-1 Steam Flow.	Alarm.	15 sec	TISL-1	TAS-1	Alarm.
TAH-2 HI TEMP RECYCLE GAS COMP INLET	Temperature Of Recycle Gas At Compressor Inlet Is Too High--Check Cooler E-2 Coolant Flow.	Alarm.	15 sec.	TISH-2	TAS-2	Alarm.
TAH-3 HI TEMP RECYCLE GAS COMP OUTLET	Temperature Of Recycle Gas At Cooler E-3 Outlet Is Too High--Check Coolant Flow.	Alarm.	15 sec	TISH-3	TAS-3	Alarm.
XAH/L-1 HI/LO COAL CONCEN'TION SLURRY FEED	Concentration Of Coal In Slurry Feed Is Too High Or Too Low.	Alarm.	15 sec	XSH/L-1	XAS-1	Alarm.

APVK/sw
2/10/78
Proj. 6148-50
Rev. 3/30/78

TABLE V

M79-26
-40

COMPUTER SCAN POINTS

```
$JOB  EXE CRDSK (CRD) TO READ PILOT PLANT DAT CARDS
$ASS RAD PP1
$EXE CRD,LMF
001R77-01              48.0              MV 00  0  0002 ADC ZERO REF -5/50 MV
002R77-02           30304. -26768.       MV 00  0  0012 ADC SPAN REF -5/50 MV
003R77-03              70.0              MV 00     0022 ADC COLD JUNCTION REF
004R77-04               9.6              MV 01    20032 ADC ZERO REF -5/10 MV
005R77-05           30528. -11072.       MV 01    20042 ADC SPAN REF -5/10 MV
006P77-01                              PSIG 40     0052 K.O  TRAP PRESSURE
007P77-02                              PSIG 40     0062 COMPRESSOR DISCHARGE PRES
008P77-03                              PSIG 40     0072 SLURRY REC PUMP DISCHARGE
009F77-01                                   40     0082 SLURRY FEED FLOW
010F77-02                                   40     0092 SLURRY RECYCLE FLOW
011F77-03                              INH2 40     0102 RECYCLE GAS FLOW
012L77-01                              INH2 40     0112 SEPARATOR LEVEL
013PD77-01                             INH2 40     0122 PRES DIF TAP 1-2
014PD77-02                             INH2 40     0132 PRES DIF TAP 2-3
015PD77-03                             INH2 40     0142 PRES DIF TAP 3-4
016PD77-04                             INH2 40     0152 PRES DIF TAP 4-5
017PD77-05                             INH2 40     0162 PRES DIF TAP 5-6
018PD77-06                             INH2 40     0172 PRES DIF TAP 6-7
019PD77-07                             INH2 40     0182 PRES DIF TAP 7-8
020PD77-08                             INH2 40     0192 PRES DIF TAP 8-9
021PD77-09                             INH2 40     0202 PRES DIF TAP 1-9
022T77-01                              DEGF 51    20212 REACTOR TEMP SEC 1 BOT
023T77-02                              DEGF 51    20222 REACTOR TEMP SEC 2 BOT
024T77-03                              DEGF 51    20232 REACTOR TEMP SEC 3 BOT
025T77-04                              DEGF 51    20242 REACTOR TEMP SEC 4 BOT
026T77-05                              DEGF 51    20252 FEED TEMP
027T77-06                              DEGF 51    20262 COOLANT TEMP E-2
028T77-07                              DEGF 51    20272 REC GAS COMPRESSOR IN
029T77-08                              DEGF 51    20282 REC GAS COMPRESSOR OUT
030T77-09                              DEGF 51    20292 REC GAS AFTERCOOLER OUT
031T77-10                              DEGF 51    20302 COOLANT TEMP E-3
032X77-01                                    0    20312 COAL CONCENTRATION
033MCR-00                                    2  1 10002 GAM RAY SCAN REACTOR OV
034MCR-01                                    2  1 10012 GAM RAY SCAN REACTOR
035MCR-02                                    2  1 10022 GAM RAY SLURRY OVER
036MCR-03                                    2  1 10032 GAM RAY SLURRY RECYCLE
037MCR-04                                    2  1 10042 GAM RAY ELEV POS
038MCR-05                                    2  1 10052 TRACER DETECTOR SEC 1
039MCR-06                                    2  1 10062 TRACER DETECTOR SEC 2
040MCR-07                                    2  1 10072 TRACER DETECTOR 4 BOT
041MCR-Z1                                    2  1 10082 TRACER DETECTOR 4 TOP
042MCR-09                                    2  1 10092 TRACER DETECTOR REC GAS
043POC-77                                    0  1 00000 BINARY SWITCHES AU77
999BS77-15                                                 TTC MOVING BIT 15
999BS77-14                                                 TTC AT TOP BIT 14
999BS77-13                                                 TTC AT BOTTOM BIT 13
999BS77-12                                                 RUN TTC BIT 12
999BS77-11                                                 SCAN/CONVERT-INPUT BIT 11
999BS77-10                                                 SLOW/FAST SCAN OF PD'S
999BS77-09                                                 TRACER INJECT BIT 9
999BS77-08                                                 END OF TEST-STATUS BIT 8
**
```

TABLE VI

Operating conditions of H—coal reactor

Gas velocity, Ft/Sec	0.04 to 0.16
Slurry velocity, Ft/Sec	0.07 to 0.18
Slurry properties (at reactor conditions)	
Viscosity, cp	0.2 to 0.5
Specific gravity, g/cc	0.6 to 0.7
Reactor slurry composition	
% Resid	25 to 30
% Solids (coal + ash)	9 to 22
% Expansion of catalyst bed	63 to 80

TABLE VII

PHYSICAL PROPERTIES OF LIQUIDS
TO BE USED IN COLD FLOW UNIT

	70°F	100°F	150°F
Viscosity (CP)			
Toluene	0.56	0.50	0.41
Kerosene	1.39	1.15	0.80
Mineral Oil	22.4	14.6	6.08
Water	1.0	1.0	1.0
Density (gm/cc)			
Toluene	0.86	0.85	0.83
Kerosene	0.79	0.78	0.77
Mineral Oil	0.85	0.84	0.82
Water	0.99	0.99	0.98

TABLE VIII

SURFACE TENSION OF FLUIDS
TO BE USED IN H-COAL UNIT, DYNES/CM

	50°F	74°F	150°F
Water	77.6	75.5	68.3
Toluene	31.7	30.8	24.5
Kerosene	30.0	28.6	24.6
Mineral Oil	34.0	32.6	29.1

DFT/ml
4/4/78

TABLE IX

CUMULATIVE SIZE DISTRIBUTION OF COAL CHAR

CUMULATIVE NUMBER AND NUMBER %
GREATER THAN STATED SIZE

Size, μm	Cumulative Number	Cumulative Number %
0	2916	100
1.1	2635	90.4
2.7	1921	65.9
3.8	1396	47.9
5.4	922	31.6
8.1	529	18.1
13.5	212	7.3
18.7	115	3.9
29.7	64	2.2
51.3	24	0.8
72.8	13	0.4
94.4	8	0.3

TABLE X

LENGTH DISTRIBUTIONS OF HDS-2A CATALYST
TO BE USED IN COLD FLOW EXPERIMENTS

Nominal Length = 1/8"

Length (Inches)	Number
Below 0.095	9
0.095-0.100	6
0.101-0.105	6
0.106-0.10	8
0.111-0.115	10
0.116-0.120	11
0.121-1.125	14
0.126-0.130	4
0.131-0.135	5
0.136-0.140	2
0.141-0.145	2
0.146-0.150	1
Above 0.150	1

Nominal Length = 3/16"

Length (Inches)	Number
Below 0.150	1
0.150-0.1575	0
0.1576-0.1650	2
0.1651-0.1725	6
0.1726-0.1800	9
0.1801-0.1875	5
0.1876-0.1950	4
0.1951-0.2025	7
0.2026-0.2100	9
0.2101-0.2175	4
0.2176-0.2250	
0.2351-0.2325	1
0.2326-0.2400	3
0.2401-0.2475	4
Above 0.2475	5

Nominal Length = 1/4"

Length (Inches)	Number
Below 0.200	2
0.200-0.210	2
0.211-0.220	7
0.221-0.230	3
0.231-0.240	2
0.241-0.250	7
0.251-0.260	5
0.261-0.270	8
0.271-0.280	7
0.281-0.290	3
0.291-0.300	3
0.301-0.310	3
Above 0.310	8

Nominal Length = 3/8"

Length (Inches)	Number
Below 0.300	3
0.300-0.315	6
0.316-0.330	5
0.331-0.345	10
0.346-0.360	8
0.361-0.375	10
0.376-0.390	7
0.391-0.405	4
0.406-0.420	9
0.421-0.435	5
0.436-0.450	4
0.451-0.465	3
Above 0.465	6

DFT/ml
6/13/78

TABLE XI

EXPERIMENTAL TESTS COMPLETED THIS YEAR

Run No.	Catalyst	Liquid	Fines, Vol%	Test No.	Liquid Flow Rate, GPM/Ft^2*	Gas Flow Rate, Ft/Sec
100	HDS-2A	Water	0	-01	22.4	0
"	L = 3/16"	"	"	-02	44.8	0
"	D = 1/16"	"	"	-03	67.2	0
"	"	"	"	-04	89.6	0
"	"	"	"	-05	22.4	0.05
"	"	"	"	-06	22.4	0.10
"	"	"	"	-07	22.4	0.15
"	"	"	"	-08	22.4	0.20
"	"	"	"	-09	44.8	0.05
"	"	"	"	-10	44.8	0.10
"	"	"	"	-11	44.8	0.15
"	"	"	"	-12	44.8	0.20
"	"	"	"	-13	67.2	0.05
"	"	"	"	-14	67.2	0.10
"	"	"	"	-15	67.2	0.15
"	"	"	"	-16	67.2	0.20
"	"	"	"	-17	89.6	0.05
"	"	"	"	-18	89.6	0.10
101	"	"	1.0	-01	22.4	0
"	"	"	"	-02	44.8	0
"	"	"	"	-03	67.2	0
"	"	"	"	-04	89.6	0
"	"	"	"	-05	22.4	0.05
"	"	"	"	-06	22.4	0.10
"	"	"	"	-07	22.4	0.15
"	"	"	"	-08	22.4	0.20
"	"	"	"	-09	22.4	0.25
"	"	"	"	-10	44.8	0.05
"	"	"	"	-11	44.8	0.10
"	"	"	"	-12	44.8	0.15
"	"	"	"	-13	44.8	0.20
"	"	"	"	-14	44.8	0.25
"	"	"	"	-15	67.2	0.05
"	"	"	"	-16	67.2	0.10
"	"	"	"	-17	67.2	0.15
"	"	"	"	-18	67.2	0.20
"	"	"	"	-19	89.6	0.05
"	"	"	"	-20	89.6	0.10

*83.3% of the flow is supplied by the recycle pump; the balance is fresh feed.

EMB/ml
8/1/78

TABLE XI

EXPERIMENTAL TESTS COMPLETED THIS YEAR
-2-

Run No.	Catalyst	Liquid	Fines, Vol%	Test No.	Liquid Flow Rate, GPM/Ft^2*	Gas Flow Rate, Ft/Sec
102	HDS-2A	Water	5	-01	30.1	0.0
"	L = 3/16"	"	"	-02	44.9	0.0
"	D = 1/16"	"	"	-03	58.3	0.0
"	"	"	"	-04	67.3	0.0
"	"	"	"	-05	76.3	0.0
"	"	"	"	-06	89.7	0.0
"	"	"	"	-07	107.3	0.0
"	"	"	"	-08	22.4	0.05
"	"	"	"	-09	22.4	0.10
"	"	"	"	-10	22.4	0.15
"	"	"	"	-11	22.4	0.20
"	"	"	"	-12	22.4	0.25
"	"	"	"	-13	44.9	0.05
"	"	"	"	-14	44.9	0.10
"	"	"	"	-15	44.9	0.15
"	"	"	"	-16	44.9	0.20
"	"	"	"	-17	44.9	0.25
"	"	"	"	-18	67.3	0.05
"	"	"	"	-19	67.3	0.10
"	"	"	"	-20	67.3	0.15
"	"	"	"	-21	67.3	0.20
"	"	"	"	-22	67.3	0.25
"	"	"	"	-23	89.7	0.05
"	"	"	"	-24	89.7	0.10
"	"	"	"	-25	89.7	0.15
"	"	"	"	-26	89.7	0.20
"	"	"	"	-27	89.7	0.25
"	"	"	"	-28	98.7	0.05
"	"	"	"	-29	98.7	0.10
200	None	Kerosene	0	-01	31.4	0.05
"	"	"	"	-02	31.4	0.10
"	"	"	"	-03	31.4	0.15
"	"	"	"	-04	31.4	0.20
"	"	"	"	-05	31.4	0.25
"	"	"	"	-06	67.3	0.05
"	"	"	"	-07	67.3	0.03
"	"	"	"	-08	67.3	0.04
"	"	"	"	-09	67.3	0.07
"	"	"	"	-10	76.3	0.03
"	"	"	"	-11	76.3	0.04
"	"	"	"	-12	76.3	0.05
"	"	"	"	-13	76.3	0.07
201	HDS-2A	"	"	-01	31.0	0.0
"	L = 3/16"	"	"	-02	44.8	0.0
"	D = 1/16"	"	"	-03	58.3	0.0
"	"	"	"	-04	67.3	0.0
"	"	"	"	-05	76.3	0.0
"	"	"	"	-06	85.3	0.0

TABLE XII

EXPERIMENTAL DATA FROM RUN 100

Test	Catalyst Bed Height (Ft)	Gamma-Ray Below Catalyst Level (cps)	Gamma-Ray Above Catalyst Level (cps)
Zero (Initial)	4.2	160	230
100-01	4.2	155	235
-02	4.6	165	240
-03	6.5	175	240
-04	8.6	190	190
-05	4.23	160	240
-06	4.4	180	250
-07	4.4	185	270
-08	4.2	180	270
-09	5.0	170	240
-10	5.2	175	250
-11	5.4	175	255
-12	5.6	175	260
-13	6.66	195	245
-14	6.8	200	260
-15	6.66	200	265
-16	6.72	200	270
-17	8.3	200	250
-18	8.3	210	250

EMB/ml
8/1/78

TABLE XIII

EXPERIMENTAL DATA FROM RUN 101

Test	Catalyst Bed Height (Ft)	Gamma-Ray Below Catalyst Level (cps)	Gamma-Ray Above Catalyst Level (cps)
Zero (Initial)	4.3	165	230
101-01	4.2	160	230
-02	4.7	165	235
-03	6.2	175	235
-04	8.33	190	230
-05	4.25	170	240
-06	4.27	175	260
-07	4.27	180	260
-08	4.27	190	270
-09	4.27	190	280
-10	4.7	165	240
-11	4.7	170	255
-12	4.7	185	265
-13	5.0	185	265
-14	5.3	190	275
-15	5.9	185	250
-16	5.94	190	250
-17	5.94	200	260
-18	5.94	200	265
-19	8.3	205	240
-20	8.3	210	250

EMB/ml
8/1/78

TABLE XIV

EXPERIMENTAL DATA FROM RUN 102

Test	Catalyst Bed Height (Ft)	Gamma-Ray Below Catalyst Level (cps)	Gamma-Ray Above Catalyst Level (cps)
Zero (Initial)	2.7	160	230
102-01	2.9	165	230
-02	3.1	165	235
-03	3.7	175	230
-04	4.1	180	235
-05	5.0	185	230
-06	5.4	190	230
-07	6.9	200	230
-08	2.8	173	240
-09	2.8	175	250
-10	2.8	180	260
-11	2.7	185	270
-12	2.7	190	270
-13	2.9	155	240
-14	3.1	165	250
-15	3.1	165	260
-16	3.3	170	270
-17	3.7	195	275
-18	4.2	190	240
-19	4.8	195	245
-20	5.0	200	255
-21	5.3	205	265
-22	5.1	215	275
-23	6.9	200	240
-24	6.2	210	240
-25	6.4	220	255
-26	7.2	225	265
-27	7.2	235	240
-28	6.4	210	235
-29	6.7	215	250

IAV/ml
12/15/78

TABLE XV

EXPERIMENTAL DATA FROM RUN 200

Test	Gamma-Ray (cps)
Zero (Initial)	330
200-01	365
-02	393
-03	426
-04	403
-05	414
-06	372
-07	343
-08	358
-09	385
-10	343
-11	358
-12	358
-13	395

IAV/ml
12/15/78

TABLE XVI

EXPERIMENTAL DATA FROM RUN 201

Test	Catalyst Bed Height (Ft)	Gamma-Ray Below Catalyst Level (cps)	Gamma-Ray Above Catalyst Level (cps)
Zero (Initial)	5.4	239	309
201-01	5.7	220	309
-02	6.9	234	309
-03	7.7	244	309
-04	8.4	252	308
-05	9.4	255	308
-06	10.2	261	310

IAV/ml
12/15/78

TABLE XVII

CALCULATED HOLDUPS IN CATALYST DENSE PHASE
FOR LIQUID/CATALYST TESTS, RUN 100

Test	ϵ_{C_B}	ϵ_{C_E}	$\epsilon_{l\gamma_B}$
100-01	0.49	0.43	0.46
100-02	0.45	0.37	0.49
100-03	0.32	0.31	0.68
100-04	0.24	0.23	0.76

EMB/ml
8/1/78

TABLE XVIII

CALCULATED HOLDUPS IN CATALYST DENSE PHASE
FOR THREE-PHASE TESTS, RUN 100

Test	ε_{ℓ_B}	$\varepsilon_{l\gamma_B}$	$\varepsilon_{g\gamma_B}$	V_{CD} (mm/sec)
100-05	0.49	0.44	0.07	11.9
-06	0.47	0.38	0.15	20.7
-07	0.47	0.36	0.17	32.0
-08	0.49	0.35	0.16	45.7
-09	0.41	0.54	0.05	11.9
-10	0.40	0.53	0.07	24.7
-11	0.38	0.57	0.05	40.8
-12	0.37	0.58	0.05	55.5
-13	0.31	0.61	0.08	8.5
-14	0.30	0.61	0.09	21.6
-15	0.31	0.59	0.10	34.1
-16	0.31	0.59	0.10	47.9
-17	0.25	0.70	0.05	14.3
-18	0.25	0.66	0.09	20.1

EMB/ml
8/1/78

TABLE XIX

CALCULATED HOLDUPS IN DILUTE PHASE
USING GAMMA-RAY SCAN DATA FOR THREE-PHASE TESTS, RUN 100

Test	ϵ_l	ϵ_g
100-05	0.99	0.01
-06	0.97	0.03
-07	0.91	0.09
-08	0.91	0.09
-09	0.99	0.01
-10	0.97	0.03
-11	0.96	0.04
-12	0.94	0.06
-13	0.99	0.01
-14	0.94	0.06
-15	0.93	0.07
-16	0.91	0.09
-17	0.97	0.03
-18	0.97	0.03

EMB/ml
8/1/78

TABLE XX

CALCULATED HOLDUPS IN CATALYST DENSE PHASE
FOR SLURRY/CATALYST TESTS, RUN 101

Test	ε_{c_B}	ε_{c_γ}	$\varepsilon_{l_{\gamma_B}}$
101-01	0.50	0.41	0.42
-02	0.45	0.38	0.49
-03	0.34	0.32	0.63
-04	0.25	0.24	0.72

EMB/ml
8/1/78

TABLE XXI

CALCULATED HOLDUPS IN CATALYST DENSE PHASE
FOR THREE-PHASE TESTS, RUN 101

Test	ϵ_{C_B}	$\epsilon_{l\gamma_B}$	$\epsilon_{g\gamma_B}$	V_{CD} (mm/sec)
101-05	0.50	0.38	0.13	8.8
-06	0.49	0.36	0.15	20.7
-07	0.49	0.34	0.17	31.7
-08	0.49	0.30	0.21	39.6
-09	0.49	0.30	0.21	51.7
-10	0.45	0.49	0.07	10.3
-11	0.45	0.46	0.09	22.3
-12	0.45	0.40	0.15	28.7
-13	0.42	0.45	0.13	45.0
-14	0.40	0.47	0.14	58.2
-15	0.36	0.56	0.08	7.7
-16	0.36	0.54	0.10	19.6
-17	0.36	0.50	0.14	28.2
-18	0.36	0.50	0.14	41.2
-19	0.25	0.66	0.08	7.1
-20	0.25	0.65	0.10	18.9

EMB/ml
8/1/78

TABLE XXII

CALCULATED HOLDUPS IN CATALYST DILUTE PHASE
FOR THREE-PHASE TESTS, RUN 101

Test	ϵ_l	ϵ_g
101-05	0.99	0.01
-06	0.94	0.06
-07	0.94	0.06
-08	0.91	0.09
-09	0.89	0.11
-10	0.99	0.01
-11	0.96	0.04
-12	0.93	0.07
-13	0.93	0.07
-14	0.90	0.10
-15	0.97	0.03
-16	0.97	0.03
-17	0.94	0.06
-18	0.93	0.07
-19	0.99	0.01
-20	0.97	0.03

EMB/ml
8/1/78

TABLE XXIII

CALCULATED HOLDUPS IN CATALYST DENSE PHASE
FOR LIQUID/CATALYST TESTS, RUN 102

Test	ε_{cB}	$\varepsilon_{c\gamma_\delta}$	$\varepsilon_{l\gamma_{\delta B}}$
102-01	0.46	0.37	0.45
-02	0.42	0.37	0.45
-03	0.36	0.31	0.47
-04	0.32	0.28	0.55
-05	0.26	0.26	0.71
-06	0.24	0.23	0.74
-07	0.19	0.18	0.77

IAV/ml
12/15/78

TABLE XXIV

CALCULATED HOLDUPS IN CATALYST DENSE PHASE
FOR THREE-PHASE TESTS, RUN 102

Test	ε_{CB}	$\varepsilon_{l}\zeta_{B}$	$\varepsilon_{g}\chi_{B}$	V_{CD} (mm/sec)
102-08	0.47	0.39	0.12	9.2
-09	0.47	0.38	0.13	21.9
-10	0.47	0.36	0.15	32.2
-11	0.49	0.31	0.19	42.1
-12	0.49	0.29	0.21	51.9
-13	0.45	0.50	0.02	13.6
-14	0.42	0.50	0.05	26.1
-15	0.42	0.50	0.05	40.6
-16	0.40	0.53	0.05	55.0
-17	0.36	0.50	0.12	60.0
-18	0.32	0.58	0.08	8.5
-19	0.28	0.63	0.06	24.2
-20	0.26	0.63	0.07	37.4
-21	0.25	0.64	0.08	50.8
-22	0.26	0.59	0.12	58.4
-23	0.19	0.75	0.02	13.7
-24	0.21	0.68	0.07	22.4
-25	0.21	0.66	0.10	34.9
-26	0.18	0.68	0.10	46.9
-27	0.18	0.65	0.13	55.2
-28	0.21	0.60	0.07	7.3
-29	0.20	0.69	0.08	21.3

EMB/ml
12/15/78

TABLE XXV

CALCULATED LIQUID/GAS HOLDUPS IN REACTOR
FOR LIQUID/GAS TESTS, RUN 200

Test	ϵ_{l_V}	ϵ_{g_V}
200-01	0.89	0.12
-02	0.82	0.18
-03	0.74	0.26
-04	0.80	0.20
-05	0.77	0.23
-06	0.88	0.12
-07	0.96	0.04
-08	0.92	0.08
-09	0.84	0.16
-10	0.96	0.04
-11	0.92	0.08
-12	0.92	0.08
-13	0.82	0.18

IAV/ml
12/15/78

TABLE XXVI

CALCULATED HOLDUPS IN CATALYST DENSE PHASE
FOR LIQUID/CATALYST TESTS, RUN 201

Test	ε_{c_B}	$\varepsilon_1\gamma_B$
201-01	0.47	0.32
-02	0.38	0.59
-03	0.34	0.61
-04	0.32	0.59
-05	0.28	0.66
-06	0.26	0.68

IAV/ml
12/15/78

TABLE XXVII

EXPERIMENTAL RICHARDSON-ZAKI INDEX

Test	n
100	2.3
101	2.1
102	3.1
201	2.9

EMB/ml
9/22/78

TABLE XVIII

CALCULATED RICHARDSON-ZAKI INDEX

	Case I	Case II
Water	2.58	2.45
Kerosene	2.80	2.73

Case I: d ≡ cylinder diameter.

Case II: D ≡ equivalent spherical diameter.

IAV/ml
12/15/78

TABLE XXIX

MEASUREMENTS OF PHYSICAL PROPERTIES OF H-COAL LIQUIDS: VISCOSITY

Laboratories Contacted	Technique	Results
1) Exxon Research and Engineering	Rotating cylinder (H. K. Bruss Rheo Verfahrenstechnik GMBH)	Instrument not readily available for outside use.
2) Core Labs	Rolling ball	Technique limited to Newtonian behavior and temperatures below 350°F.
3) Amoco Production	Rolling ball	Same limitations as core lab.
	Rotating cylinder (Fann Model 50C viscometer).	Limited to temperatures less than 500°F and pressures less than 1000 psi.
4) Fann Instrument Corporation	Iron bob magnetically forced up and down in a cylinder containing the sample (Fann 5STDL consistometer).	Limited to temperatures below 500°F.
5) Battelle Labs	Iron bob magnetically forced up and down in a cylinder containing the sample.	Preliminary proposal submitted.

IAV/ml
9/30/77

Figure 1

Construction schedule of the FDU

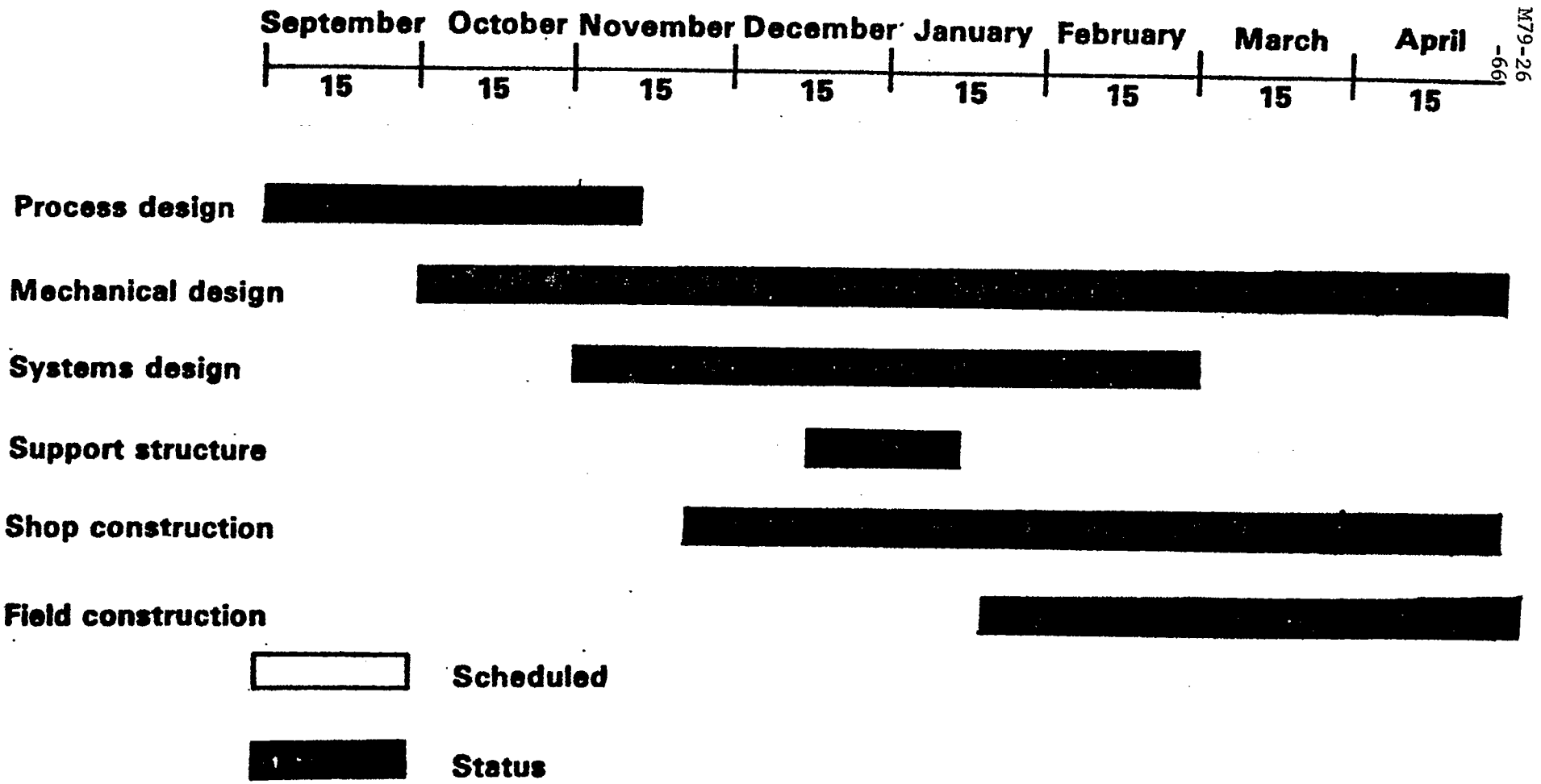

M79-26
-669

Figure 2

SCHEMATIC DIAGRAM OF THE FLUID DYNAMICS UNIT

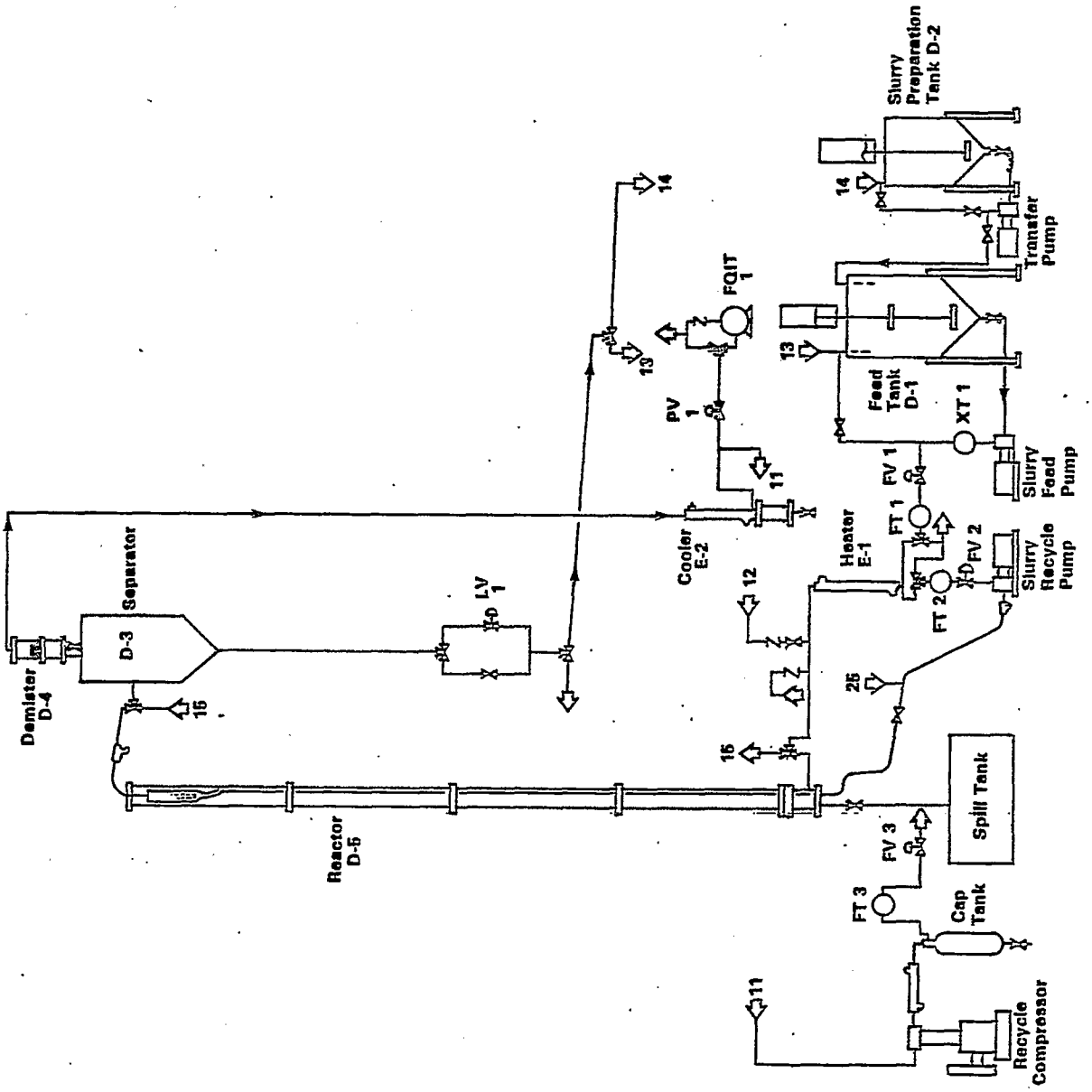

Figure 3

REACTOR DESIGN

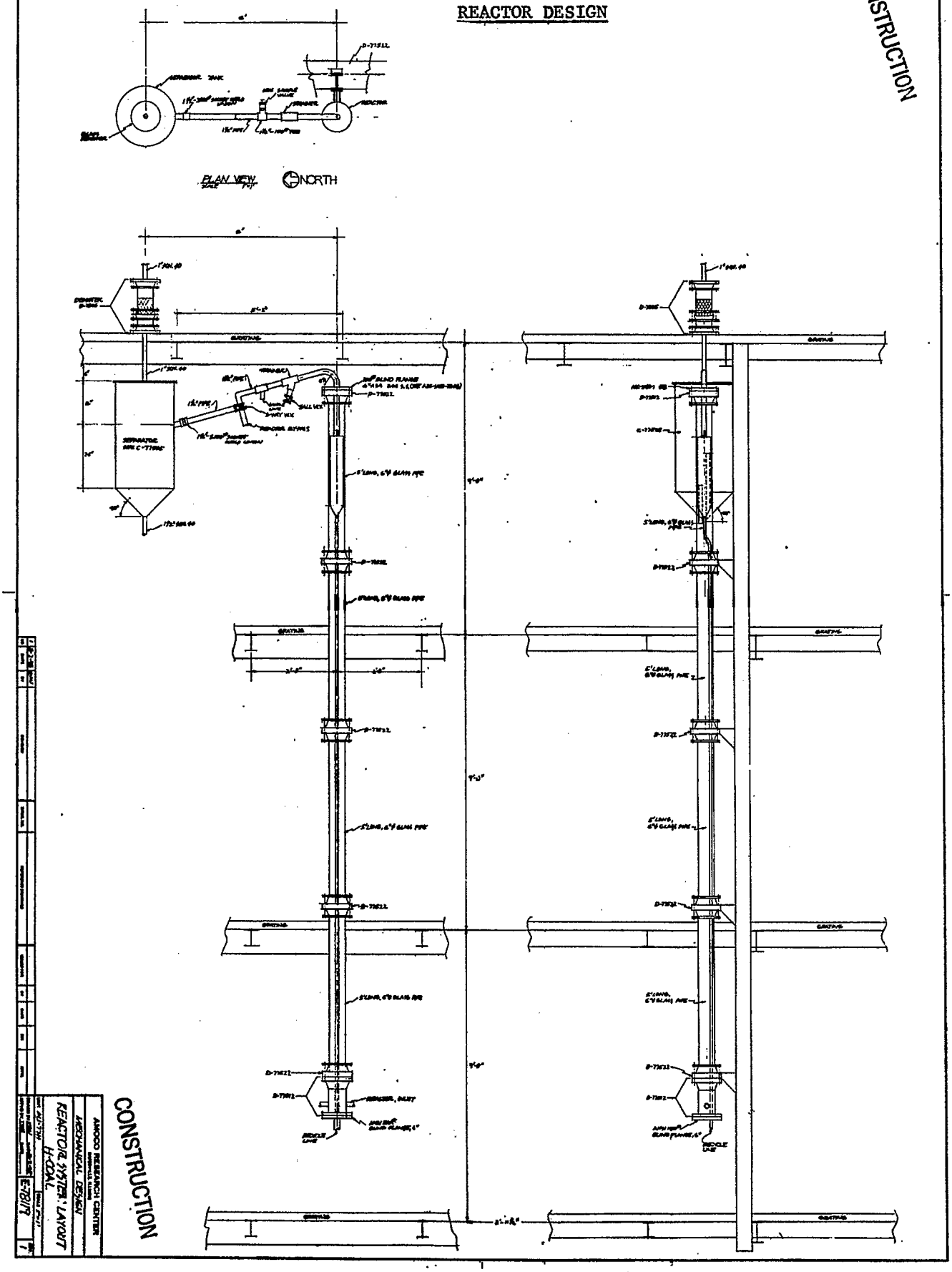

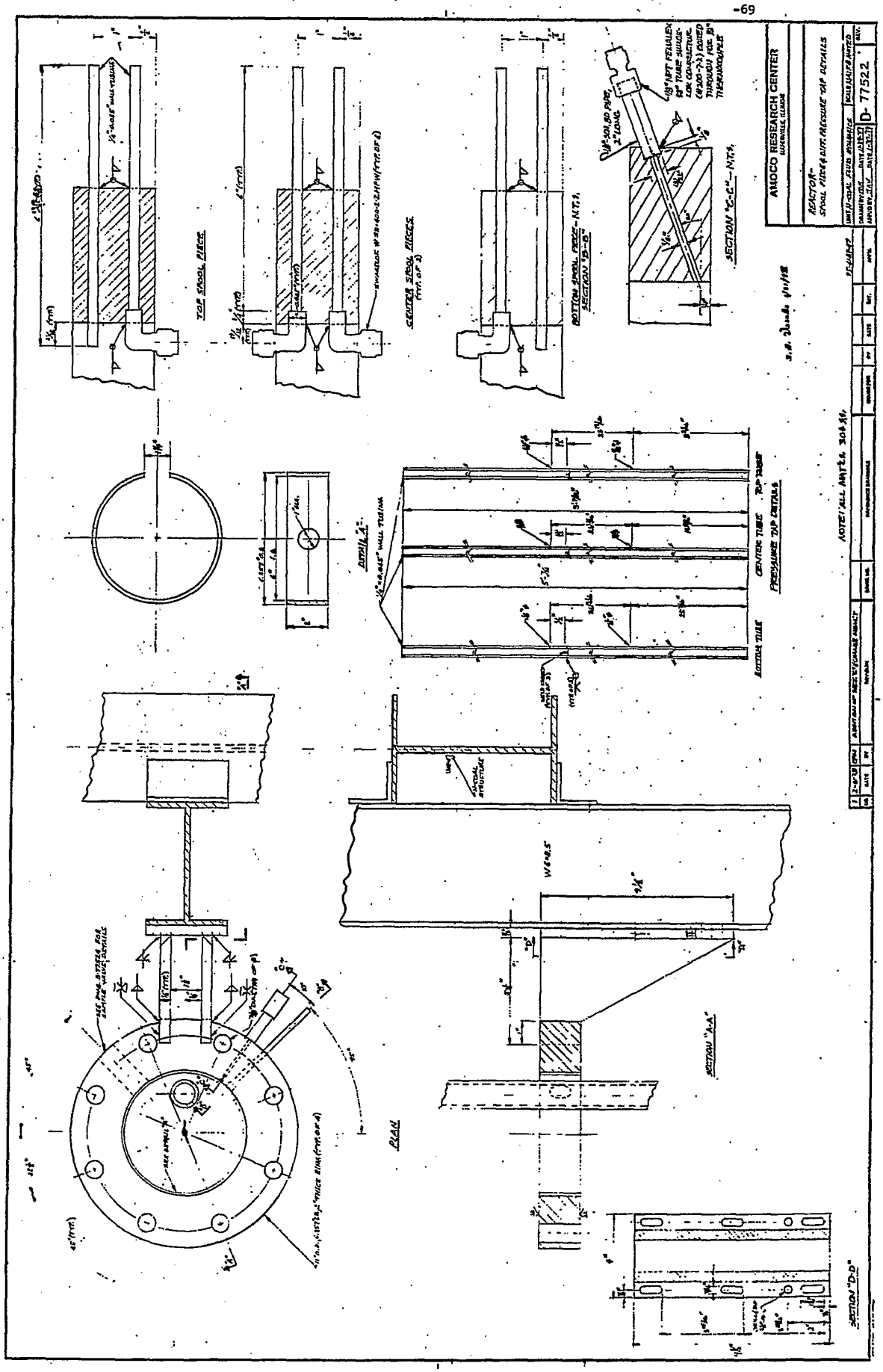
AMOCO RESEARCH CENTER
NAPERVILLE, ILLINOIS
REACTOR-
STEAM SLEEVE AND PRESSURE TAP DETAILS
D-77522
TOP STEAM PIECE
CENTER STEAM PIECE
BOTTOM STEAM PIECE
SECTION "C-C"
SECTION "A-A"
SECTION "B-B"
PLAN
CENTER TUBE TOP DETAILS
PRESSURE TAP DETAILS
BOTTOM TUBE
NOTE: ALL PARTS S.S. 304 SS.

Figure 4

Figure 5

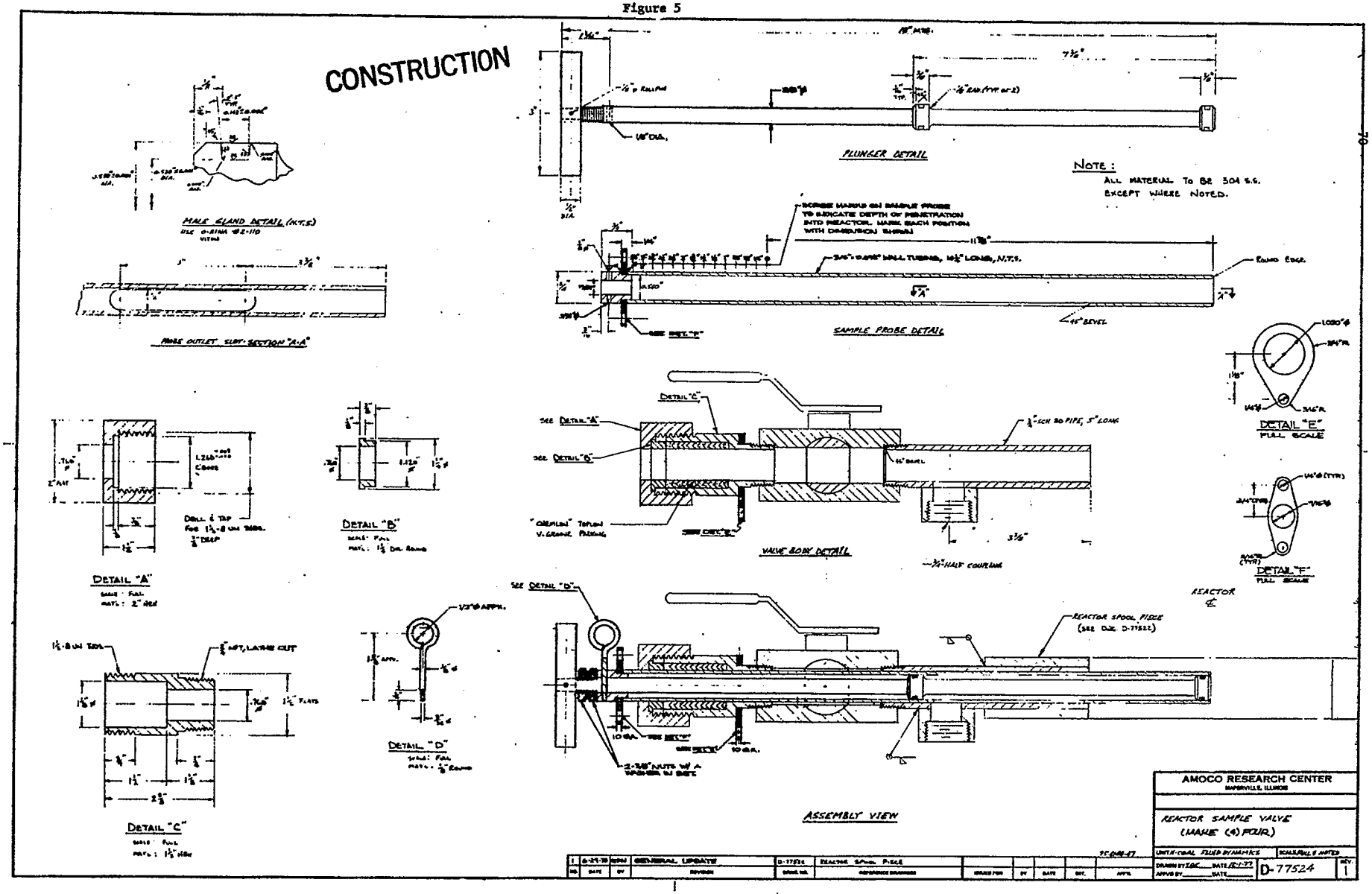

M79-26
70

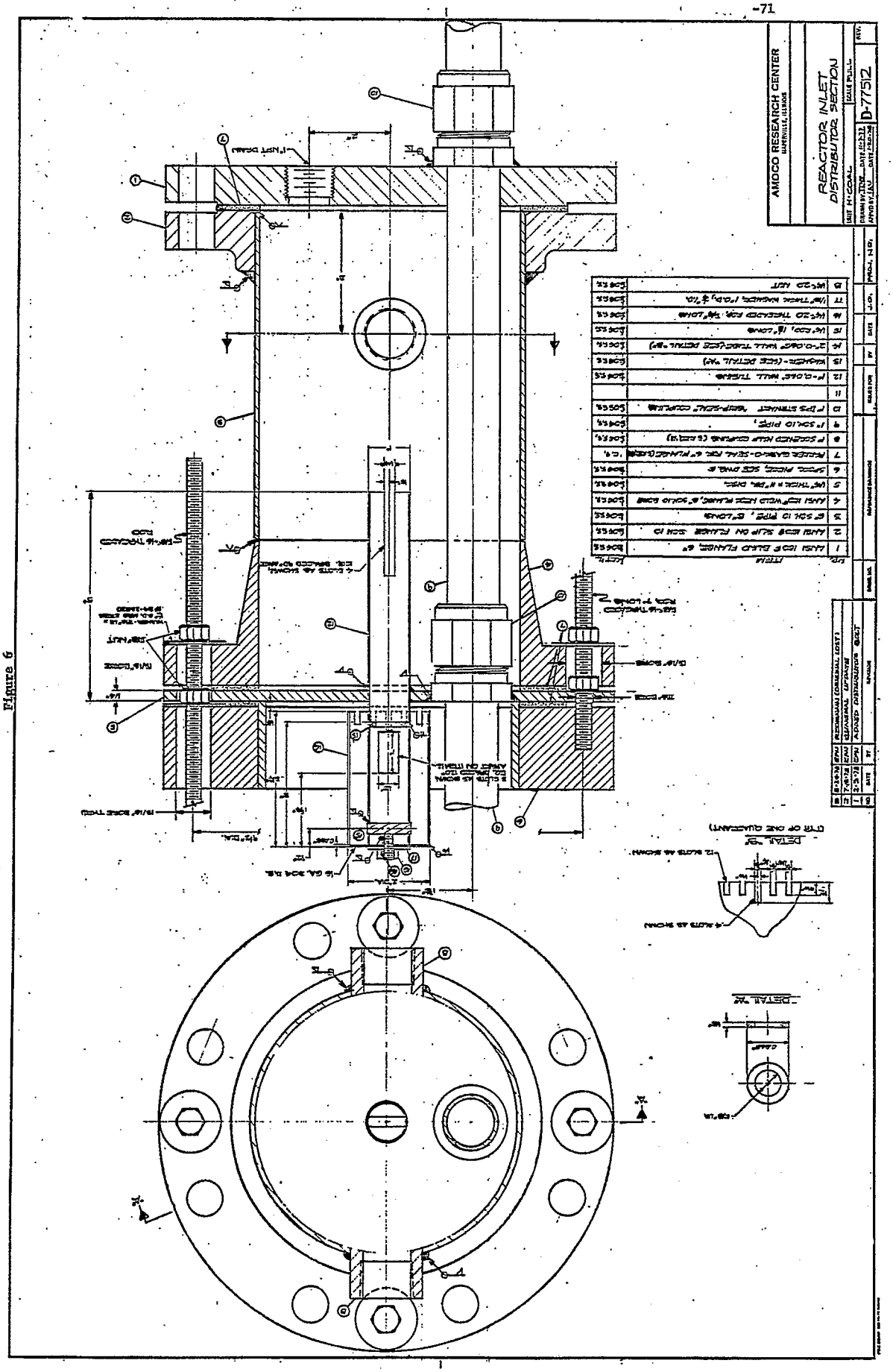
AMOCO RESEARCH CENTER
REACTOR INLET
DISTRIBUTOR SECTION
D-77512
ITEM
DETAIL "W"
DETAIL "M"
(TYP OF ONE QUADRANT)

Figure 6

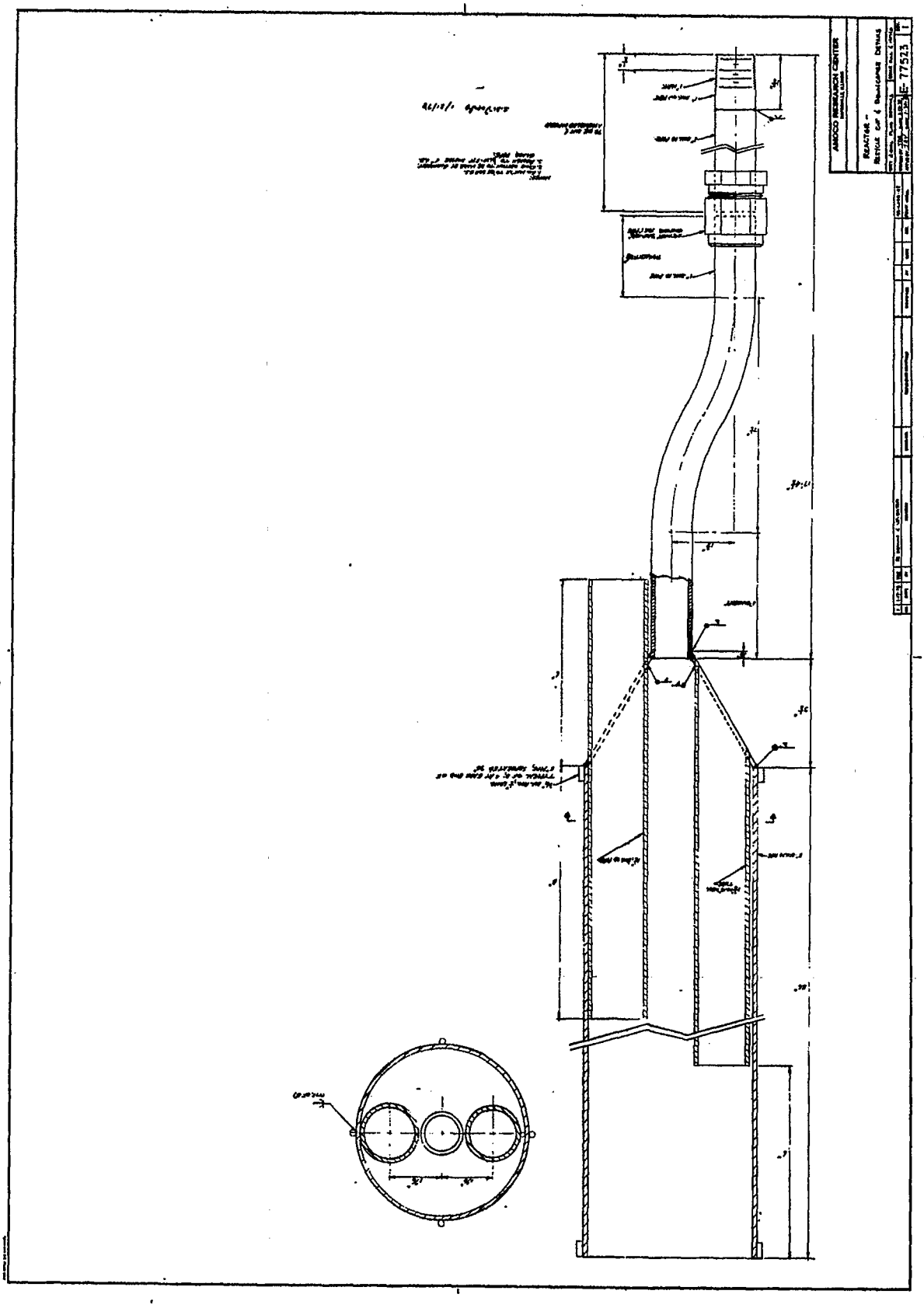

Figure 7

Figure 8

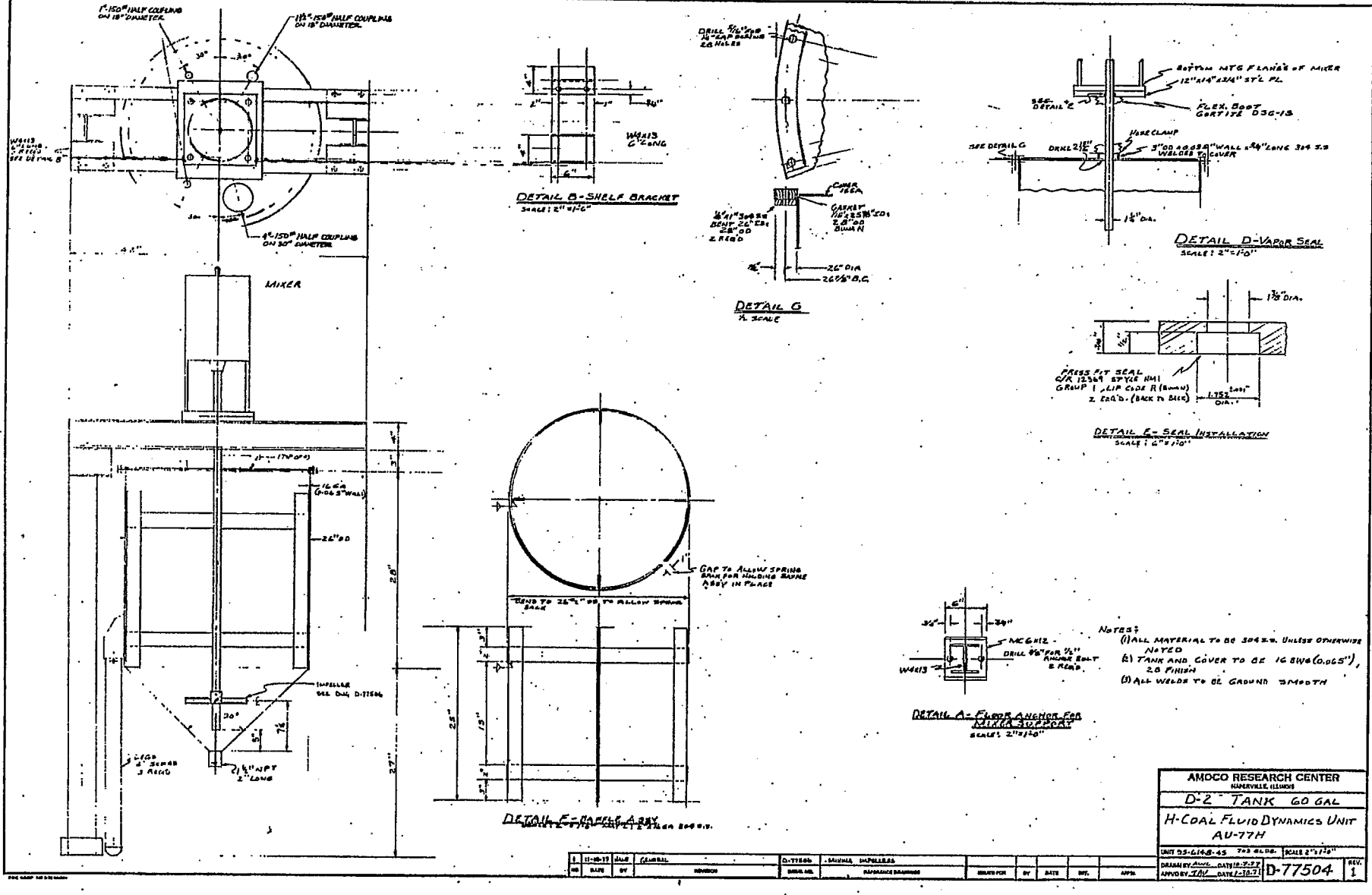
MIXER
DETAIL B-SHELF BRACKET
DETAIL G
DETAIL D-VAPOR SEAL
DETAIL E-SEAL INSTALLATION
DETAIL F-BAFFLE ASSY
DETAIL A-FLOOR ANCHOR FOR MIXER SUPPORT
NOTES:
(1) ALL MATERIAL TO BE 304 S.S. UNLESS OTHERWISE NOTED
(2) TANK AND COVER TO BE 16 SWG (0.065"), 2B FINISH
(3) ALL WELDS TO BE GROUND SMOOTH
AMOCO RESEARCH CENTER
NAPERVILLE, ILLINOIS
D-2 TANK 60 GAL
H-COAL FLUID DYNAMICS UNIT
AU-77H
D-77504
REV. 1

Figure 9.

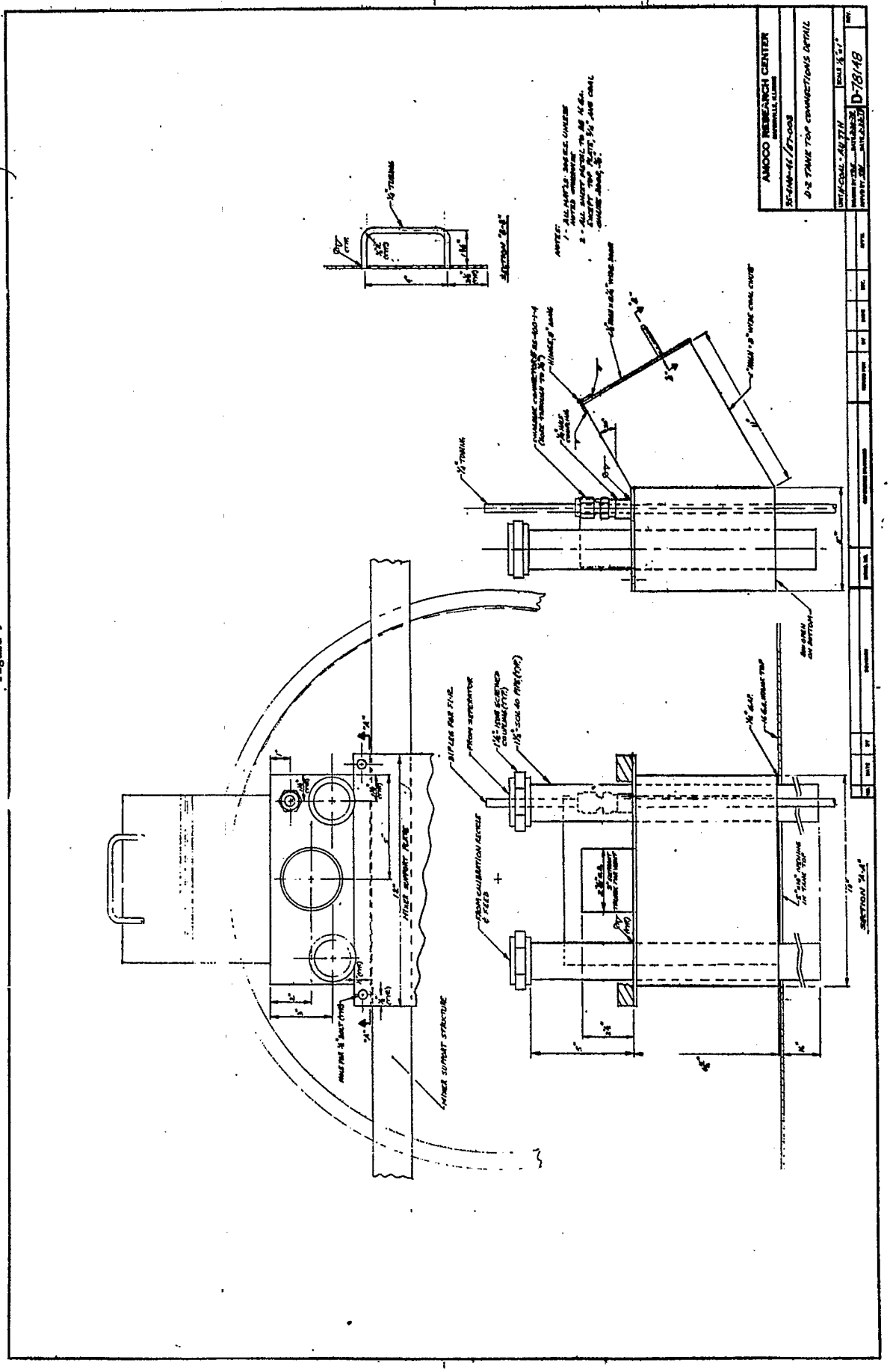

Figure 9